Cell Reports
Methods

Article

Activation-neutral gene editing of tonsillar CD4 T cells for functional studies in human *ex vivo* tonsil cultures

Graphical abstract

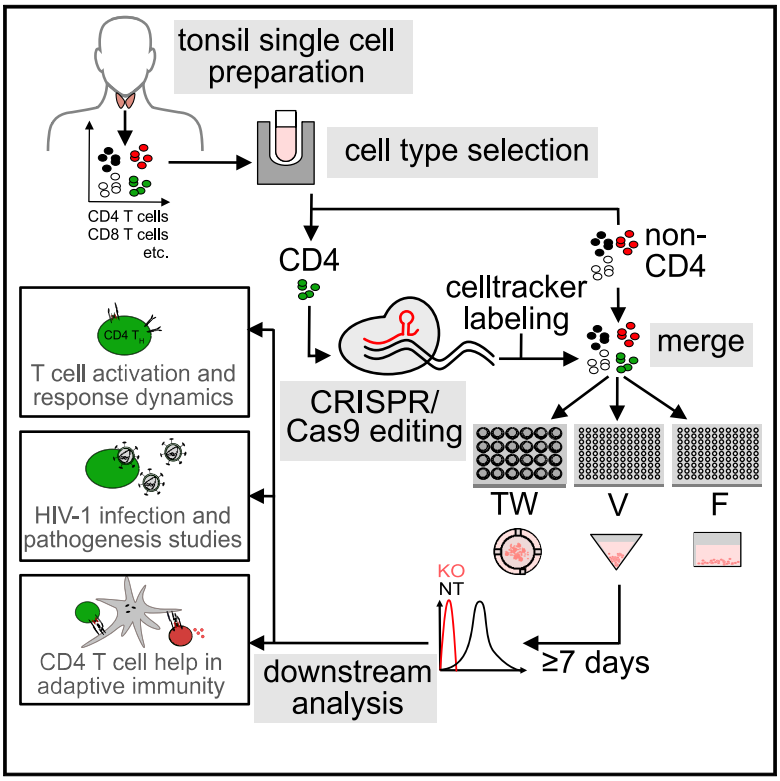

Highlights

- ediTONSIL is a versatile gene editing workflow for tonsillar CD4 T cells
- Optimized RNP nucleofection enables highly efficient editing
- ediTONSIL preserves tissue-resident properties of the edited cells
- Underlying molecular mechanisms can be dissected by studying reintegrated edited cells

Authors

Katharina Morath, Lopamudra Sadhu, Gerhard Dyckhoff, Madeleine Gapp, Oliver T. Keppler, Oliver T. Fackler

Correspondence

oliver.fackler@med.uni-heidelberg.de

In brief

Morath et al. present a workflow for highly efficient gene editing of tonsil CD4 T cells without disturbing their physiological functions and unique properties. Reintegration of edited and labeled cells in their physiological cell environment enables mechanistic dissection of cell-cell interactions, e.g., in adaptive immunity or during HIV infection.

Morath et al., 2024, Cell Reports Methods *4*, 100685
January 22, 2024
https://doi.org/10.1016/j.crmeth.2023.100685

CellPress

Cell Reports Methods

CellPress
OPEN ACCESS

Article

Activation-neutral gene editing of tonsillar CD4 T cells for functional studies in human *ex vivo* tonsil cultures

Katharina Morath,[1] Lopamudra Sadhu,[1] Gerhard Dyckhoff,[2] Madeleine Gapp,[3] Oliver T. Keppler,[3,4] and Oliver T. Fackler[1,5,6,*]

[1]Department of Infectious Diseases, Integrative Virology, University Hospital Heidelberg, Im Neuenheimer Feld 344, 69120 Heidelberg, Germany

[2]Department of Otorhinolaryngology, Head and Neck Surgery, University Hospital Heidelberg, Im Neuenheimer Feld 400, 69120 Heidelberg, Germany

[3]Max von Pettenkofer Institute and Gene Center, Virology, National Reference Center for Retroviruses, Ludwig-Maximilians-Universität München, Pettenkoferstraße 9a, 80336 Munich, Germany

[4]German Centre for Infection Research (DZIF), Partner Site München, Munich, Germany

[5]German Centre for Infection Research (DZIF), Partner Site Heidelberg, Heidelberg, Germany

[6]Lead contact

*Correspondence: oliver.fackler@med.uni-heidelberg.de

https://doi.org/10.1016/j.crmeth.2023.100685

MOTIVATION CD4 T cells are central players of adaptive immunity that rapidly change activation states in response to exogenous T cell receptor (TCR) stimulation. While molecular processes in activated human CD4 T cells from peripheral blood are well studied, resting CD4 T cells are refractory to gene editing transduction and transfection methods without prior activation. Knowledge on the molecular biology of truly resting CD4 T cells in their tissue environment is therefore lacking. We present here the culture and editing workflow ediTONSIL that allows for gene editing of tissue-resident CD4 T cells without compromising their activation state or immunological function. Reintegration in their natural cell environment enables molecular mechanistic analyses of this cell type in their native/physiological tissue context.

SUMMARY

The molecular and immunological properties of tissue-resident resting CD4 T cells are understudied due to the lack of suitable gene editing methods. Here, we describe the *ex vivo* culture and gene editing methodology ediTONSIL for CD4 T cells from human tonsils. Optimized CRISPR-Cas9 RNP nucleofection results in knockout efficacies of over 90% without requiring exogenous activation. Editing can be performed on multiple cell types in bulk cultures or on isolated CD4 T cells that can be labeled and reintroduced into their tissue environment. Importantly, CD4 T cells maintain their tissue-specific properties such as viability, activation state, or immunocompetence following reassembly into lymphoid aggregates. This highly efficient and versatile gene editing workflow for tonsillar CD4 T cells enables the dissection of molecular mechanisms in *ex vivo* cultures of human lymphoid tissue and can be adapted to other tonsil-resident cell types.

INTRODUCTION

Adaptive immune reactions involve fine-tuned, complex, and dynamic interactions between different cell types that define the remarkable potency of our immune system. In the case of CD4 T cells, interactions with antigen-presenting cells (APCs) that display MHC-II-restricted specific antigenic peptides in the context of close cell-cell conjugates (immunological synapse) drive CD4 T cell activation, proliferation, and differentiation to elicit effector function that includes helper functions to B and CD8 T cells toward humoral and cytotoxic immune responses, respectively.[1] These APC-effector interactions take place in lymphoid organs and tissue architecture, composition, and density are essential parameters for efficacy and outcome of these reactions. Despite this essential impact of the tissue environment, most studies on CD4 T cell function employ CD4 T cells from readily available peripheral blood, which display activation and differentiation states that are markedly distinct from that of tissue-resident CD4 T cells. An alternative approach is the use of small animal models (mostly

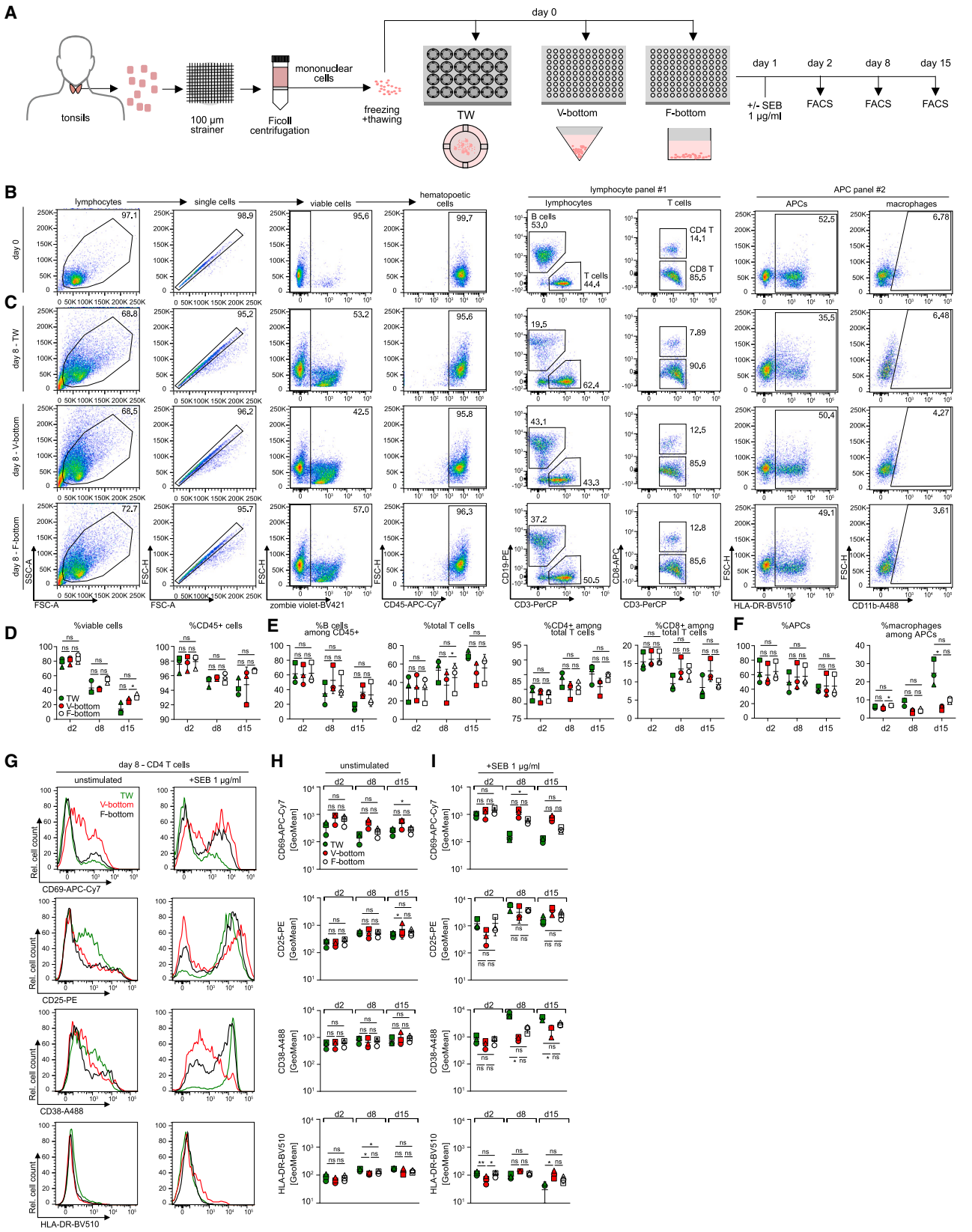

(legend on next page)

mouse), in which complex immune reactions can be studied. While these models provide fundamental insight, they also have important limitations with respect to human pathogenesis as they differ in tissue composition, the spectrum of cell surface markers to identify cell populations, life span and exposure to a complex immune-stimulatory environment.[2] These differences are particularly relevant for studies of pathogen-host interactions such as HIV infection as even transgenic or humanized mouse models do not fully mirror the complex pathogenesis induced by the infection in humans.[3,4] To overcome this limitation, organotypic *ex vivo* cultures of lymphoid tissue explants were developed and cultures of human tissue organ proved most useful. Grown as tissue blocks (human lymphoid histoculture [HLH])[5–12] and in suspension (human lymphoid aggregate culture [HLAC]),[9,10,13–16] human tonsil tissue is permissive to HIV-1 infection and mirrors hallmarks of HIV pathogenesis such as CD4 T cell depletion. In important contrast to peripheral blood CD4 T cells that require activation for productive HIV infection, tonsil CD4 T cells are fully permissive although they are phenotypically resting and do not proliferate.[5] Of note, the original version of HLH retained the ability to elicit adaptive antibody responses to recall antigen[7,17,18] and a recent optimization of cell purification and reassembly also improved the immunological features of HLACs, allowing the testing of vaccine candidates.[19,20]

The key limitation in this organotypic and immunocompetent cell culture system is the lack of methodology for targeted gene editing of specific cell types, which currently precludes detailed molecular dissection of cell function in this tissue-like context. Most available methods for gene editing of primary human lymphocytes require prior cell activation for efficient delivery of viral vectors, expression of transgenes, or sufficiently high transfection rates.[21–23] These approaches are typically associated with high cytotoxicity and editing rates that require subsequent isolation of edited cells. Moreover, these editing approaches require prior cell activation and analyses are therefore limited to the second stimulation of cells that had returned to a phenotypical resting state after a first round of activation. We recently introduced a CRISPR-Cas9 RNP nucleofection approach for peripheral blood CD4 T cells that resulted in highly efficient gene editing without compromising the resting state of these cells.[21] In this study, we adapted this protocol to tissue-resident cells in *ex vivo* tonsil cultures that are first characterized with respect to different culture setups and define the ediTONSIL workflow that enables the activation-neutral editing of bulk and isolated tonsil cell populations. Reintegration of these cells in their physiological cell context enables the molecular dissection of complex immune cell interactions in these organotypic cultures.

RESULTS

Optimizing culture conditions of *ex vivo* tonsil suspension cultures

The viability of *ex vivo* tonsil cultures is currently limited to 2–3 weeks.[5,19,24] To establish optimized conditions, we compared the impact of different culture conditions on cell viability, activation/differentiation, and response to stimulation. Tonsil tissue from healthy donors that underwent routine tonsillectomy or tonsillotomy were dispersed through a cell strainer for subsequent isolation of mononuclear cells (Figure 1A). At this step, cells can be either plated for immediate culture or frozen in aliquots for future use. For comparison, we plated cells in transwells (TW) or V- or F-bottom 96-well plates for subsequent phenotypic characterization by flow cytometry (Figure 1A). Cell viability was assessed by staining with the dead-cell dye zombie violet (over 95% viable cells at day 0) and cell type composition was determined by the detection of specific cell surface markers (Figure 1B). Expectedly, cell viability decreased over time, reaching approximately 20% after 15 days of culture. This decline was independent of the culture format (Figure 1D). With respect to specific cell populations, the relative amount of T cells slightly increased with time at constant CD4 vs. CD8 T cell ratios at the expense of APCs. The only notable impact of the culture format was a marked enrichment of macrophages among all APCs in TW cultures (Figure 1F). Activation of CD4 T cells with staphylococcal enterotoxin B (SEB) superantigen triggered potent cell surface exposure of the activation markers CD69, CD25, and CD38 within 7 days, while HLA-DR surface levels remained largely unaltered (Figures 1G–1I; Figures S1A–S1E). While the activation pattern was similar in all three culture conditions, exposure of the early activation marker CD69 was more transient and induction of surface CD38 more pronounced in TW cultures.

Figure 1. Comparison of cell culture plates for human tonsil cell culture

(A) Schematic of the experimental setup. Cell suspensions were prepared from human tonsils, frozen, and thawed for culture in three different cell culture plate systems, 24-well transwell culture (TW), 96-well V-bottom (V-bottom), or 96-well F-bottom (F-bottom) plates at 10×10^6 cells/mL. Cell composition was analyzed on day 2, day 8, and day 15 post seeding by flow cytometry analysis. Activation response of CD4 T cells in the different setups was measured 1, 7, and 14 days post addition of SEB at 1 μg/mL by flow cytometry.

(B) Representative dot plots and gating strategy for identification of cell populations within tonsil bulk cell cultures at day 0, using two antibody cocktails for characterization of lymphoid cells (panel #1) and myeloid cells (panel #2).

(C) Representative dot plots at day 8 of culture for TW, V-bottom, and F-bottom setups.

(D–F) Quantification of (B) and (C) for three tonsils in TW (green), V-bottom (red), or F-bottom (white) setups.

(G) Representative histograms of CD4 T cell surface activation marker expression of CD25, CD69, CD38, and HLA-DR on day 8 of culture with (+SEB 1 μg/mL) or without (unstimulated) exogenous activation.

(H and I) Quantification of CD69, CD25, CD38, and HLA-DR signal on CD4 T cells without (H) or with (I) exogenous activation as shown in (G) for three tonsils in TW (green), V-bottom (red), or F-bottom (white) setups. Shown are means with SD. Each symbol represents one donor. Statistical significance was assessed by repeated measures one-way ANOVA for all datasets except where data were not normally distributed and statistical testing was performed using Friedman test (% macrophages among APCs, F; CD38 expression [unstimulated/+SEB] and CD25 expression in the unstimulated condition, H). ns, $p > 0.05$; *$p < 0.05$; **$p < 0.01$; ***$p < 0.001$; ****$p < 0.0001$).

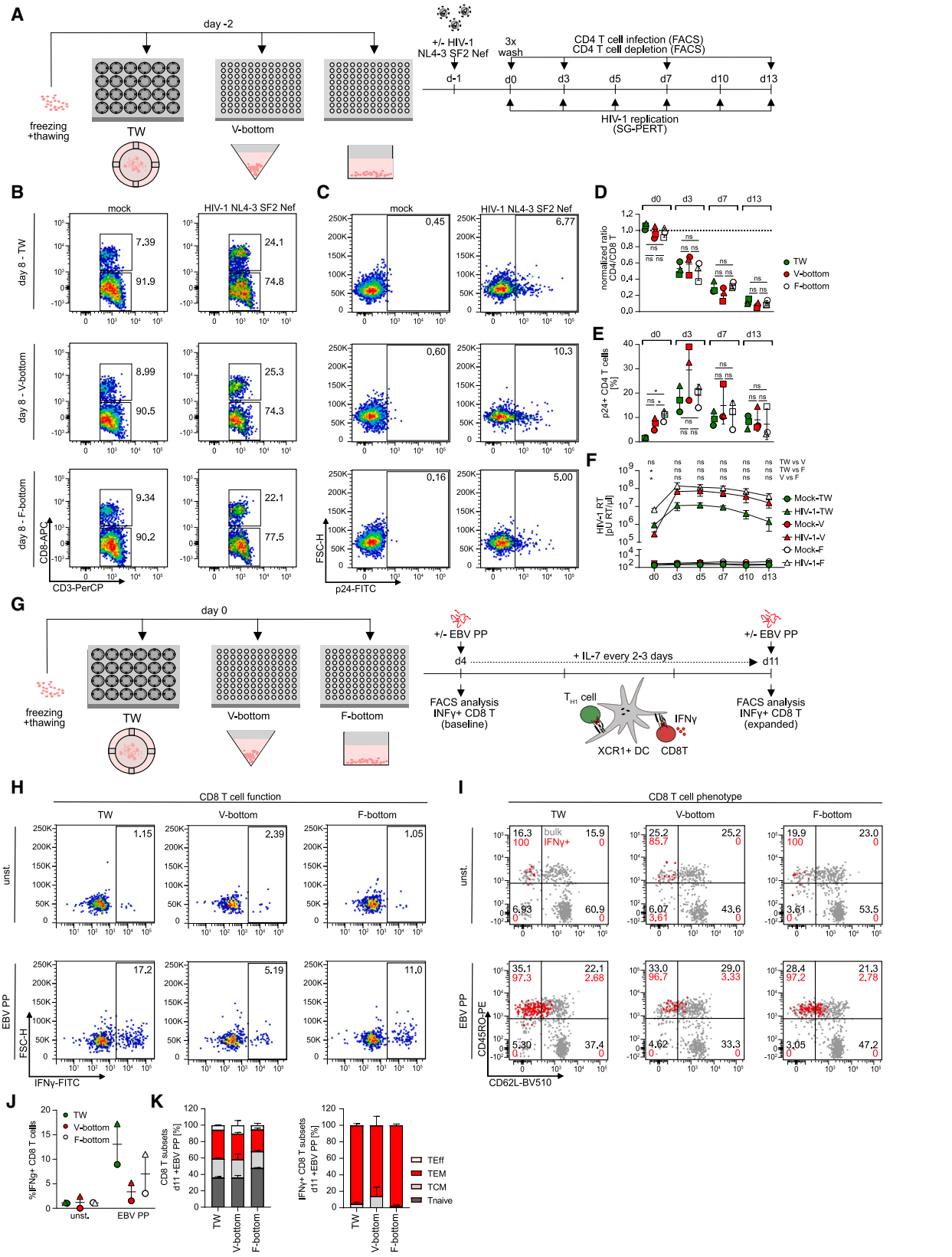

(legend on next page)

We next conducted a function characterization of *ex vivo* tonsil cultures under these different conditions. Since HIV-1 typically replicates efficiently in *ex vivo* tonsil cultures and induces the specific depletion of CD4 T cells that is characteristic for AIDS pathogenesis,[5,7,25,26] we first analyzed their permissivity for HIV-1 infection. Following plating, cultures were infected with the full-length, replication-competent HIV-1 variant NL4.3 $SF2_{nef}$ 1 day later and HIV-1 replication and CD4 T cell depletion were quantified over time by assessing the activity of the viral enzyme reverse transcriptase in the cell culture supernatant (SG-PERT assay[27,28]), determining the number of productively infected cells by intracellular staining for the viral capsid protein p24, and defining the ratio of CD4 vs. CD8 T cells by flow cytometry (Figures 2B–2F). As indicated by the reduction in CD4 T cells paralleled by a relative increase in CD8 T cells, CD4 T cell depletion upon HIV-1 infection was observed with comparable magnitude and kinetics in all three culture conditions. The frequency of productively infected, $p24^+$ cells reached a peak 3 days post infection (dpi) and then declined, but V-bottom cultures tended to allow the detection of higher frequencies of productively infected cells among viable cells (Figure 2E). Finally, virus replication in the culture as determined by the SG-PERT assay also rapidly increased in the first dpi and then slowly declined with time but the virus titers observed in TW cultures were markedly lower compared with those in the other culture conditions (Figure 2F).

To assay the immune competence of these cultures, we probed their ability to mount CD4 T cell help to CD8 T cells in response to presentation of a recall antigen by $XCR1^+$ dendritic cells (DCs)[29–32] (Figure 2G; Figures S1F–S1P). To this end, cultures were treated with a pool of peptides derived from Epstein-Barr virus (EBV), a very common and lifelong infection in the general population that can trigger efficient CD4 and CD8 T cell responses.[33–35] The presence and expansion of reactive memory cells was then probed 1 week later by the quantification of interferon gamma (INFγ)-producing CD8 T cells upon peptide restimulation. We observed expansion of $INF\gamma^+$ CD8 T cells in response to EBV peptides in all culture conditions but this effect was clearly more pronounced in TW and F-bottom cultures and V-bottom cultures only allowed for residual expansion of $INF\gamma^+$ CD8 T cells (1.5%/5.2% IFNγ+ CD8 T cells for two tonsils compared with above 3.0/8.9 and 11.0%/17.2% in F-bottom and TW cultures for the same tonsils, respectively) (Figures 2H and 2J). The subset distribution of total or CD8 T $INF\gamma^+$ cells, however, was comparable in all culture conditions (mean of 36.0%–47.8% T_{naive}, 20.3%–23.1% T_{CM}, 26.5%–35.1% T_{EM} and 5.4%–10.5% T_{Eff} cells among total CD8 T cells across the culture setups compared with 1.7%–13.9% T_{CM} and 86.1%–98.4% T_{EM} among IFNγ+ CD8 T cells) (Figures 2I and 2K). Of note, prior depletion of CD4 T cells from these cultures abrogated the induction of $INF\gamma^+$ CD8 T cells, indicating that CD4 T cell help is critical for this expansion (Figures S1M–S1P). The culturing format thus has important implications for the functional properties of these cultures with all three culture systems supporting HIV-1 replication yet superior preservation of immunocompetence in TW and F-bottom cultures, which are therefore more suitable for the analysis of complex immune reactions.

Establishment of ediTONSIL gene knockout in bulk tonsil cultures

We next attempted to perform gene editing of tonsil cells, here termed ediTONSIL, by example of the chemokine receptor CXCR4 that serves as an essential co-receptor for entry of X4-tropic HIV-1 strains and is abundantly expressed on all major immune cell populations. To this end, thawed bulk tonsil cells were nucleofected with CRISPR-Cas9 RNP complex and cultured for 7 days. Knockout (KO) was assessed on the protein level by flow cytometry, which enabled the analysis of KO efficiency in distinct cell (sub)populations and differentiation states (Figures 3A–3G). Among the lymphocyte populations, B cells and CD4 and CD8 T cells displayed highly efficient KO of the *cxcr4* gene compared with a non-targeting (NT) RNP control within 7 days (Figures 3C–3F; mean B cell CXCR4 surface level for NT 9793.0 ± 1338.7 arbitrary units

Figure 2. Different culture setups for human tonsil cells support HIV-1 infection to similar extend but show distinct preservation of immunocompetency

(A) Schematic of the experimental setup. Cryopreserved human tonsil cells were thawed and seeded in 24-well transwell (TW), 96-well V-bottom or 96-well F-bottom cell culture plates 1 day prior to infection with 1.5×10^5 BCU per 2×10^6 cells using HIV-1 NL4.3 $SF2_{nef}$ virus. On subsequent days, HIV-1 infection was characterized by analyzing CD4 T cell depletion by a decreased CD4/CD8 T cell ratio and CD4 T cell infection by intracellular flow cytometry staining for HIV-1 capsid protein (p24) and last, detection of newly produced HIV-1 virions in the culture supernatant by SG-PERT.

(B and C) Representative dot plots showing CD4 and CD8 T cells subgated from CD3 T cells as well as p24 signal in CD4 T cells for the three culture setups.

(D and E) Quantification of (B) and (C) for three tonsils for the respective harvesting timepoints cultured in TW (green), V-bottom (red), or F-bottom (white) setups. Shown are means with SD. Each symbol represents one donor.

(F) SG-PERT analysis of HIV-1 RT activity in the supernatant for mock or HIV-1 infected cultures in TW (green), V-bottom (red), or F-bottom (white) setups. Of note, the higher culture volume in TW plates is a confounding factor for lower RT activity/μL. Shown are means with SD of three tonsils per data point.

(G) Schematic of the experimental setup for analysis of EBV-specific memory CD8 T cell reactivation in tonsil cultures. Briefly, cells were thawed and seeded in 24-well transwell (TW) or 96-well V- or F-bottom plates as depicted. On day 4, EBV peptide pool was added together with interleukin (IL)-7 for 7 days. On day 4 and day 11, baseline and expanded EBV-specific CD8 T cells, respectively, were identified by production of IFNγ following stimulation with the EBV peptide pool.

(H) Representative dot plots of CD8 T cells in bulk tonsil cell cultures on day 11 of culture with (EBV PP) or without (unst.) EBV peptide pool.

(I) Characterization of memory subsets based on expression of CD45RO and CD62L among total (gray) or superimposed IFNγ+ (red) CD8 T cells on day 11 following peptide stimulation of tonsil cells cultured with (EBV PP) or without (unst.) EBV peptide pool for 7 days.

(J) Quantification of (H) for two tonsils per condition. Shown are means with range.

(K) Quantification of (I) for total or IFNγ+ CD8 T cells on day 11 in EBV PP-stimulated cultures. T_{Eff} = T effector cells, T_{EM} = effector memory cells, T_{CM} = central memory cells, T_{naive} = naive T cells. Statistical significance of CD4 T cell infection and SG-PERT data were assessed by repeated measures one-way ANOVA (E) and (F). The CD4 T cell depletion data in (D) were normalized and Friedman test was used for analysis. ns, $p > 0.05$; *$p < 0.05$; **$p < 0.01$; ***$p < 0.001$; ****$p < 0.0001$.

(legend on next page)

[AU] vs. KO 166.3 ± 41.7, CD4 T cells 2996.3 ± 341.8 vs. 171.3 ± 26.8 and CD8 T cells 2321.0 ± 328.4 vs. 103.6 ± 31.4) irrespective of the memory differentiation state of CD4 or CD8 T cells (Figures 3G–3M; CD4 T T_{CM} CXCR4 surface level mean for NT 5977.0 ± 1556.3 AU vs. KO 114.3 ± 3.2, T_{naive} 9543.7 ± 1419.5 vs. 230.3 ± 66.0 and T_{EM} 8065.0 ± 1392.8 vs. 173.0 ± 22.3; CD8 T T_{CM} 5051.3 ± 1527.6 vs. 99.9 ± 8.1, T_{naive} 4606.3 ± 2177.5 vs. 137.7 ± 14.4 and T_{EM} 4049.0 ± 765.2 vs. 117.8 ± 70.4) and KO efficiency did not require further exogenous stimulation by SEB (Figures S2A–S2E). Among myeloid cells, macrophages and DCs, although far less abundant in tonsil cultures than lymphocytes, were edited with similar efficiency (macrophage CXCR4 surface levels: NT 3845.7 ± 742.4 AU vs. KO 165.2 ± 68.3; DC CXCR4 surface levels: 8464.0 ± 640.9 vs. 67.4 ± 21.1; Figures S2F–S2J). Such highly efficient KO was consistently obtained with tonsil cultures from different donors; however, the extent by which the procedure impaired cell viability varied between cells from different donors. Reduction in cell viability was accompanied by an upregulation of the T cell activation markers CD25 and CD69, indicating general stress induced by the nucleofection (Figures 3N–3Q). Nevertheless, KO of *cxcr4* in bulk tonsil cultures was functional and prevented productive HIV-1 infection, virus-induced CD4 T cell depletion, and virus replication (Figures 3R–3X). Altogether, these results establish that genes can be efficiently knocked out in bulk tonsil cultures; however, the results also reveal that this approach is associated with significant cytotoxicity and unspecific CD4 T cell activation.

Establishment of ediTONSIL gene KO in tonsil CD4 T cells

We reasoned that nucleofection conditions would need to be optimized for each cell population in tonsil cultures to limit cytotoxicity. Since there is no approach that renders nucleofection specific for a distinct cell subset in a complex heterogeneous mix of different cells, we attempted to improve cell viability following gene editing by isolating specific cell populations from tonsil cultures for editing. An additional requirement that gene editing of tissue-resident cells should fulfill is that subsequent reuniting these cells with the unedited tonsil cells allows for reconstituting of the original cell composition and function of the culture to support the precise molecular dissection of cell-cell interactions in the natural tissue context (Figure 4A). Focusing on CD4 T cells, we first established positive selection of CD4 T cells by magnetic beads (magnet-assisted cell sorting, MACS) as the most efficient method for cell isolation (CD4 T cell purity 94.5%/55.6% for two donors after negative isolation vs. 91.7%/85.6% for the same tonsils after positive selection, respectively and 16.5%/6.1% vs. 2.5%/1.5% CD4 T cells left in the non-CD4 cell fraction; Figures S3A–S3D; Table S1) which enabled us to faithfully reconstitute tonsil cultures following isolation and add back (Figure 4B). Importantly, efficiency of the positive isolation with respect to CD4 T cell depletion from the non-CD4 fraction is underestimated by negative gating for CD4 T cells based on CD3 and CD8 staining since a large fraction of the residual population does not express CD4, likely representing unconventional T cells and further validating the efficiency of the CD4 positive selection (Figures S3A–S3H). Of

Figure 3. Gene editing of bulk tonsil cells by CRISPR-Cas9 nucleofection is highly efficient in all major tonsil cell populations and across T cell differentiation states

(A) Schematic of experimental setup. Tonsil cells were thawed, nucleofected with non-targeting or *cxcr4* RNP complex, and cultured in 96-well F-bottom plates for 1 week until analysis of KO efficiency in distinct cell populations by flow cytometry.

(B) Representative dot plots and gating strategy for identification of lymphocyte subsets among tonsil cell cultures.

(C) Representative histograms showing CXCR4 surface expression on B cells and CD4 and CD8 T cells on day 7 post nucleofection with CXCR4-targeting RNP (c*xcr4* KO) with superimposed histograms for the non-targeting RNP (NT) condition and isotype control.

(D)-(F) Quantification of (C) for NT or c*xcr4* KO in B cells, CD4 or CD8 T cells. Each dot represents one tonsil. Shown are means with SD.

(G) Representative dot plots and gating strategy for identification of memory subsets based on CD45RA and CD62L expression among CD4 and CD8 T cells in tonsil cell cultures.

(H and K) Representative histograms showing CXCR4 surface expression on central memory (T_{CM}), naive (T_{naive}) and effector memory (T_{EM}) CD4 (H) or CD8 (K) T cell subsets on day 7 post nucleofection with c*xcr4*-targeting RNP (CXCR4 KO) with superimposed histograms for the non-targeting RNP (NT) condition and isotype control.

(I and L) Distribution of memory subsets among CD4 (I) and CD8 (L) T cells for the NT or c*xcr4* KO condition.

(J and M) Quantification of (H) and (K) for NT or *cxcr4* KO conditions in the respective memory subsets. Each dot represents one tonsil. Shown are means with SD.

(N) Relative surface expression of CXCR4 on c*xcr4* KO or NT tonsil cells on day 7 post nucleofection, calculated by normalizing the MFI in c*xcr4* KO conditions to the NT control.

(O–Q) Frequency of viable cells (O) or surface expression of CD25 (P) and CD69 (Q) on CD4 T cells among NT or *cxcr4* KO cultures on day 7, normalized to non-nucleofected (no nucl.) cells, respectively.

(N)–(Q) Each dot represents one tonsil. Shown are means with SD. Tonsils were cultured in 24-well transwell plates.

(R) Schematic of experimental setup for analysis of HIV-1 infection in c*xcr4* KO tonsil cultures. Briefly, tonsil cells were thawed, nucleofected with CRISPR-Cas9 RNP complex as indicated and infected with HIV-1 NL4.3 $SF2_{nef}$ at 1.5×10^5 BCU per 2×10^6 cells 7 days later by addition of the virus to the cultures. On the following day (d0), cells were washed 3x and infection was assessed by analysis of CD4 T cell infection and depletion by flow cytometry analysis upon final harvest and production of HIV-1 virions in the supernatant by SG-PERT throughout the infection course.

(S and T) Representative dot plots showing CD4 and CD8 T cells subgated from CD3 T cells (S) as well as p24 signal in CD4 T cells (T) in NT or *cxcr4* KO mock or HIV-1 infected conditions, respectively on day 7 post infection.

(U and V) Quantification of (S) and (T) for two tonsils with the ratio of CD4 vs. CD8 T cells in (U) normalized to the mock condition for NT or *cxcr4* KO, respectively.

(W and X) HIV-1 RT activity in the supernatant of mock or HIV-1 infected NT or *cxcr4* KO cultures at indicated timepoints. Cells were cultured in 96-well V-bottom plates. Statistical significance was assessed by paired t test for comparison of two groups in (D), (E), (F), (I), (J), (L), (M), or by Wilcoxon test in (N) (normalized data). Data in (O)–(Q) were normalized and Friedman test was used for comparison of more than two groups. ns, $p > 0.05$; *$p < 0.05$; **$p < 0.01$; ***$p < 0.001$; ****$p < 0.0001$.

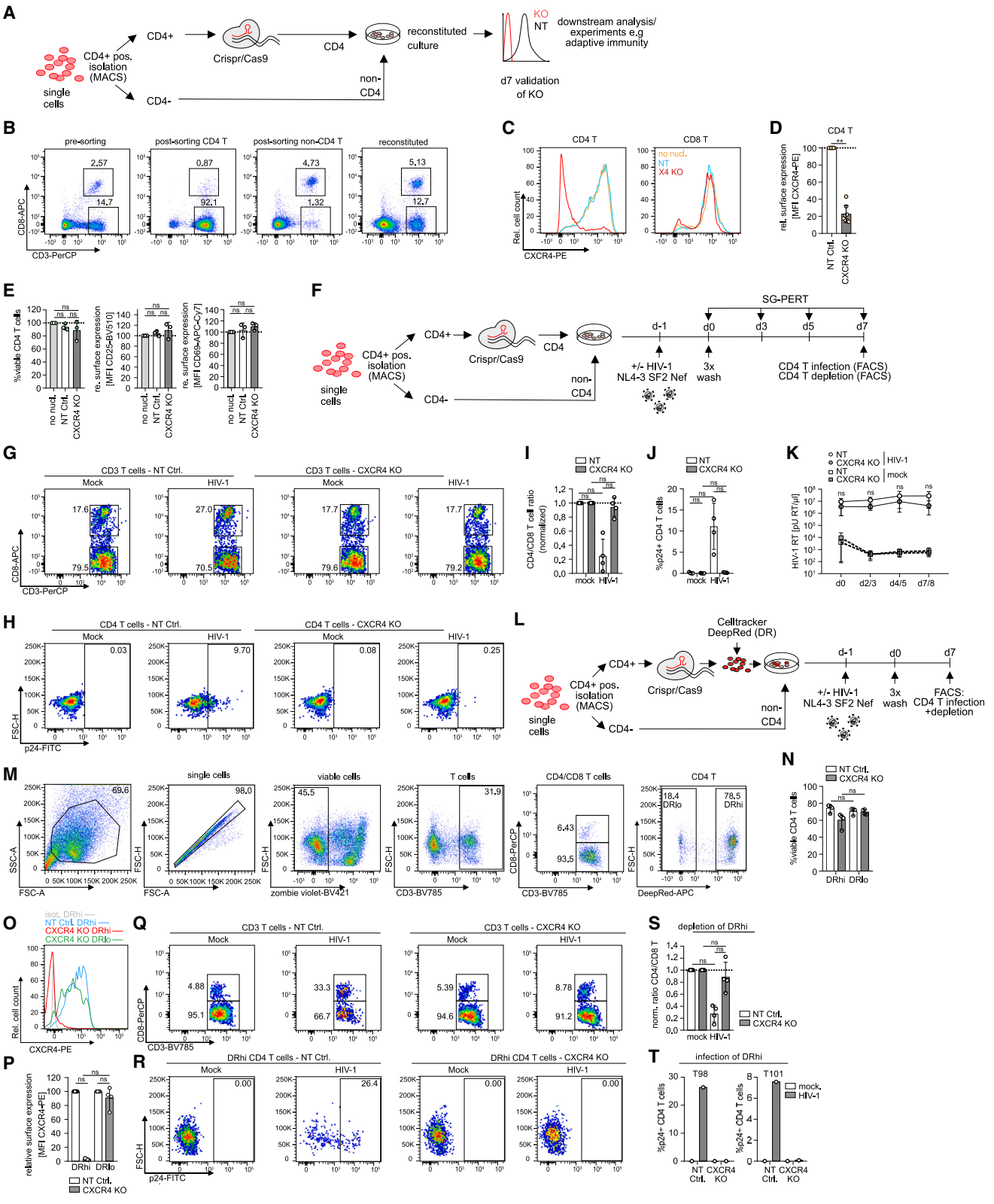

(legend on next page)

note, the positive isolation method did not affect viability, activation or susceptibility to HIV-1 infection (Figures S3I–S3T). Nucleofection of isolated CD4 T cells with *cxcr4*-specific CRISPR-Cas9 RNP complexes and immediate reconstitution resulted in highly efficient reduction of CXCR4 on CD4 T cells within 7 days post nucleofection (mean of 22.4% ± 10.1% CXCR4 surface expression left for KO normalized to NT CD4 T cells, Figures 4C and 4D). Importantly, this procedure did not affect CD4 T cell viability or activation state and exogenous cytokine supplementation was thus not required to enhance survival, likely explained by the presence of T cell survival factors that are already provided by the tonsil microenvironment[36,37] (Figure 4E; Figures S4A–S4F). Similar KO efficiency was obtained in positively vs. negatively isolated CD4 T cells, excluding adverse effects of the positive isolation strategy, e.g., by residual magnetic particles on CD4 T cells during nucleofection. Moreover, independently prepared RNP complexes yielded comparable KO efficiencies, validating the reproducibility of the workflow (Figures S4G–S4I). Infecting tonsil cultures that were reconstituted after *cxcr4* gene editing in CD4 T cells with HIV-1 (Figure 4F) revealed that the removal of the entry co-receptor strongly reduced virus-induced depletion of CD4 T cells (~5% relative CD4 T cell reduction in in *cxcr4* KO vs. ~75% in the NT condition) and fully abrogated virus replication in these cultures to a similar extent as treatment with the HIV-1 entry-inhibitor T20 (Figures 4G–4K; Figures S4J–S4O). Since the tonsillar CD4 T cells were permissive to HIV-1 infection in the absence of exogenous activation, this important functional property of tissue-resident CD4 T cells was not impaired by the editing procedure.

The KO procedure was highly efficient as only ~10% of CD4 T cells in the reconstituted cultures were precluded from editing. These represent residual CD4 T cells present in the non-CD4 T cell fraction that could not be removed during initial cell separation (Figure 4B; Figures S3E–S3H). While not sufficient to drive appreciable HIV-1 replication in *cxcr4* KO cultures, this residual population may exert immune functions that are relevant for other scenarios. We therefore tested if labeling of the isolated and gene-edited CD4 T cell population allows for phenotypically distinguishing edited and unedited cell populations in reconstituted tonsil cultures after embedding of CD4 T cells (Figure 4L). Staining of gene-edited CD4 T cells with DeepRed celltracker prior to culture reconstitution followed by 1 week of culture indeed allowed the identification of gene-edited (DeepRed high [DRhi]) and unedited (DeepRed low [DRlo]) populations with

Figure 4. CD4 T cells can be specifically targeted for gene editing by CRISPR-Cas9 RNP nucleofection in tonsil culture by magnetic cell isolation and reconstitution

(A) Schematic of experimental setup. Briefly, tonsil cells were thawed and subjected to positive magnetic cell isolation of CD4 T cells. Magnetic beads were then removed from CD4 T cells prior to CRISPR-Cas9 RNP nucleofection and CD4 T cells were merged with the negative, non-CD4 T cell fraction, forming the reconstituted culture. Seven days post nucleofection, efficiency of the KO was assessed by flow cytometry.

(B) Representative dot plots showing CD4 and CD8 T cell frequencies among bulk cells prior to CD4 sorting (pre-sorting) and CD4 fraction after sorting (post-sorting CD4 T) and non-CD4 fraction after sorting (post-sorting non-CD4 T) as well as the reconstituted culture post merging of CD4 and non-CD4 fraction (reconstituted).

(C) Representative histograms of CXCR4 expression on CD4 and CD8 T cells on day 7 following CD4 T cell isolation, nucleofection and merging with non-CD4 T cells. Shown is the CXCR4 surface signal on non-nucleofected (no nucl.), NT control (NT), or *cxcr4* KO (X4 KO) cultures.

(D) Quantification of CXCR4 on CD4 T cells for eight tonsils. CXCR4 signal was normalized to the NT condition for each tonsil. Tonsil cells were cultured in 24-well transwell or 96-well V-bottom plates.

(E) Frequency of viable CD4 T cells and surface expression of CD25 and CD69 among NT or *cxcr4* KO CD4 T cells on day 7 for three tonsils, normalized to non-nucleofected cells, respectively. Tonsil cells were cultured in 24-well transwell plates. (D) and (E) Each dot represents one donor. Shown are means with SD.

(F) Schematic of experimental setup to assess HIV-1 infection in tonsil cultures with edited CD4 T cells. Briefly, tonsil cells were thawed and CD4 T cells were isolated and nucleofected prior to merging with non-CD4 T cells. On day 7 post nucleofection, cultures were infected with HIV-1 NL4.3 $SF2_{nef}$ at 1.5×10^5 BCU per 2×10^6 cells and HIV-1 infection was assessed on subsequent days by analysis of CD4 T cell depletion, CD4 T cell infection by intracellular p24 staining, and production of new virions in the supernatant by SG-PERT.

(G and H) Representative dot plots showing frequencies of CD4 and CD8 T cells among tonsil CD3 T cells (G) or intracellular p24 staining among tonsil CD4 T cells (H) in mock or HIV-1 infected cultures on day 7 post infection for NT or *cxcr4* KO cultures, respectively.

(I) Quantification of (G) for four tonsils, normalized to the mock condition, respectively.

(J) Quantification of (H) for four tonsils. Tonsil cells were cultured in 24-well transwell or 96-well V-bottom plates. (I), (J) Each dot represents one donor. Shown are means with SD.

(K) SG-PERT quantification of HIV-1 RT activity in the supernatant at indicated timepoints for mock or HIV-1 infected cultures nucleofected with NT or *cxcr4* KO RNP. Shown are means with range of three donors per condition. Tonsil cells were cultured in 24-well transwell or 96-well V-bottom plates.

(L) Schematic of the experimental setup for identification of nucleofected CD4 T cells among total CD4 T cells in tonsil culture by celltracker staining.

(M) Representative dot plots and gating strategy for identification of nucleofected, celltracker DeepRed high intensity (DRhi) CD4 T cells in tonsil bulk cultures.

(N) Quantification of viable CD4 T cells among DRhi and DRlo cells in NT and *cxcr4* KO conditions for four tonsils.

(O) Representative histogram of CXCR4 expression on celltracker-stained (DRhi), *cxcr4* KO CD4 T cells with superimposed histogram of the DRhi population in the NT condition and isotype control as well as DRlo CD4 T cell population in the CXCR4 KO condition.

(P) Relative surface expression of CXCR4 on the DRhi and DRlo population in *cxcr4* KO tonsil CD4 T cells on day 7 post nucleofection, normalized to the NT control for four tonsils. Shown are means with SD.

(Q and R) Representative dot plots showing frequencies of CD4 and CD8 T cells among tonsil CD3 T cells (Q) or intracellular p24 staining among DRhi tonsil CD4 T cells (R) in mock or HIV-1 infected cultures on day 7 post infection for NT or *cxcr4* KO cultures, respectively.

(S) Quantification of the CD4 vs. CD8 T cell ratio as calculated for the DRhi population among total CD4 T cells for four tonsils, normalized to the mock condition, respectively. (N), (P), (S) Each dot represents one donor. Shown are means with SD.

(T) Quantification of R in HIV-1 infected cultures for two tonsils as depicted. Tonsil cells for celltracker experiments were cultured in 96-well V-bottom plates. Statistical significance was assessed by Wilcoxon test for comparison of two groups in (D) or by Friedman test for comparison of more than two groups in (E), (I), (K), (N), (P), and (S). For normally distributed data in (J), repeated-measures one-way ANOVA was used. ns, $p > 0.05$; *$p < 0.05$; **$p < 0.01$; ***$p < 0.001$; ****$p < 0.0001$.

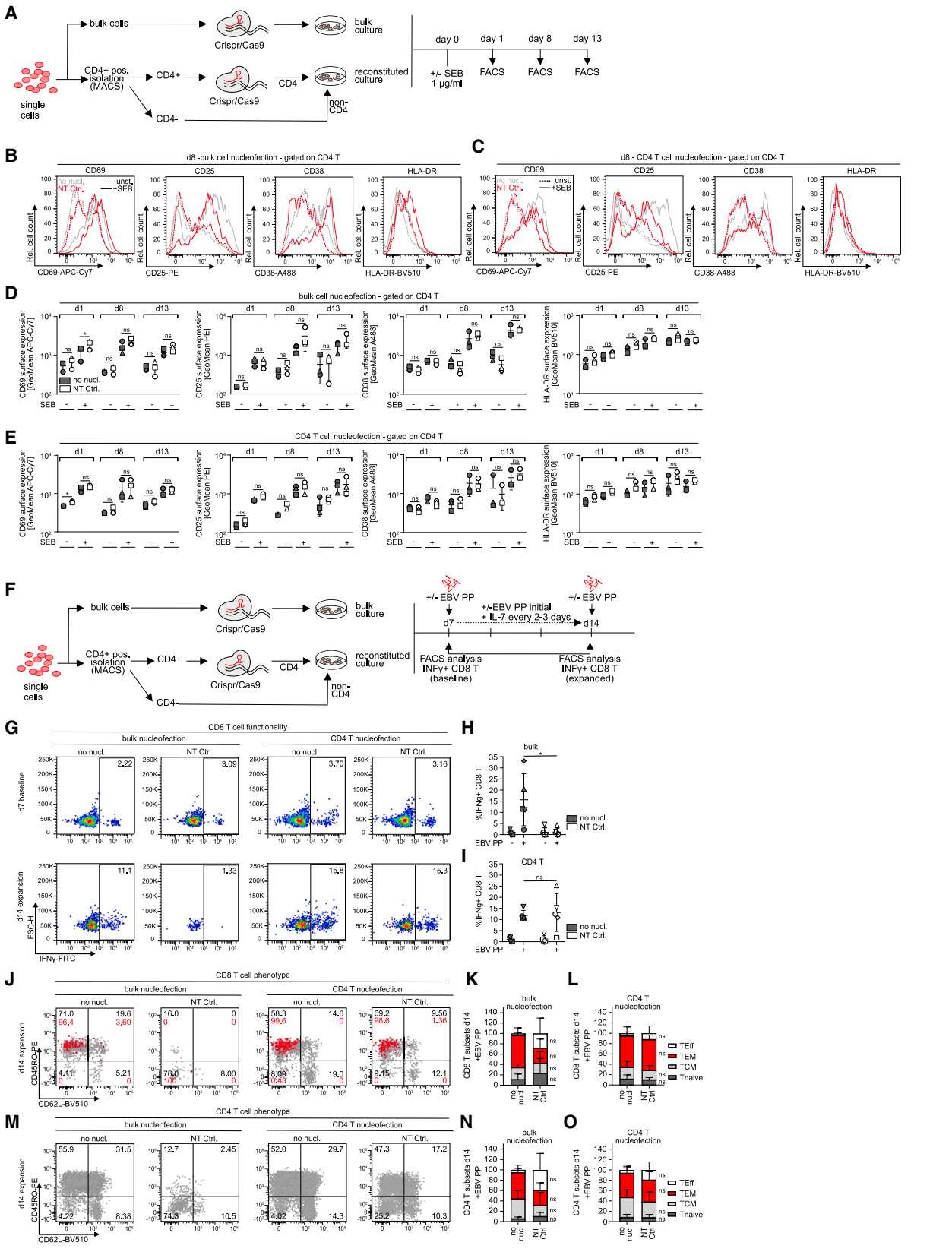

(legend on next page)

unaffected viability of celltracker-stained cells (74.2% ± 4.4% viable cells in NT DRhi CD4 T vs. 71.1% ± 3.9% in DRlo and 60.2% ± 8.3% in *cxcr4* KO DRhi CD4 T vs. 69.7% ± 3.2% in DRlo; Figures 4M and 4N). Of note, CXCR4 cell surface expression was undetectable on DRhi cells (Figures 4O and 4P), revealing that the residual $CXCR4^+$ CD4 T cell population in the experiment described above (Figure 4D) reflects the presence of unedited cells, largely consisting of CD4/CD8-negative T cells and a minor fraction of CD4 T cells that resisted positive selection. Consistently, DRhi cells were fully protected from HIV-1 infection (Figures 4Q–4T). Isolation and modification of CD4 T cells combined with subsequent reconstitution of tonsil cultures thus allows for highly efficient and activation-neutral gene editing where edited cell populations can be further labeled by celltracker staining to unambiguously identify cells of interest while enabling direct comparison with unedited cells in the same condition.

Gene editing to study complex adaptive immune reactions

In contrast to HIV-1 replication and virus-induced depletion of CD4 T cells, complex immune reactions such as mounting of recall CD8 T cell responses (Figures S1F–S1P) depend on complex functional interactions of several immune cell types. To address if gene editing affects the ability of cells to conduct such activities following reconstitution, we assessed next the impact of ediTONSIL on adaptive immune reactions. First, we performed RNP nucleofection on bulk tonsil cultures or on isolated CD4 T cells with subsequent reconstitution into a complex organotypic culture and assessed the response of these cultures to T cell activation by SEB (Figure 5A). Under both conditions, the analysis of cell surface activation markers revealed an efficient response of CD4 T cells to stimulation that was not significantly altered in magnitude and kinetic by the nucleofection procedure (Figures 5B–5E). We next applied the analogous experimental setting to the expansion of EBV-specific CD8 T cells in response to the EBV peptide pool (Figures 2G and 5F). While RNP nucleofection of bulk tonsil cells abrogated the ability of these cultures to expand IFNγ+ CD8 T cells, editing of isolated CD4 T cells did not impair their ability to provide help for CD8 T cell expansion in their tonsil environment (Figures 5G–5I). Consistently, the CD8 T cell subset distribution was slightly skewed toward effector cells (T_{Eff}) upon bulk nucleofection while isolated editing of CD4 T cells did not significantly affect the memory T cell subset composition of these cultures (Figures 5J–5O). EdiTONSIL of isolated tonsil CD4 T cells with subsequent embedding in the physiological cell environment thus preserves their capacity to undergo complex adaptive immune reactions.

DISCUSSION

Increasing efforts are made to study pathobiological principles and their therapeutic targeting in complex organoid and organotypic models to account for the impact of tissue environments and cell type heterogeneity at complexity levels between individual cell types (cell line or isolated primary cells) and small animal models/patient samples. In particular for lymphoid organs that predominately consist of hematopoietic cells, which are difficult to generate by iPS technology,[38,39] *ex vivo* tonsil cultures are a well-established organotypic model that proved invaluable to study complex pathogen replication and complex immune reactions *ex vivo*.[5,7,9,18–20,24,40–43] However, the full potential of this culture model for gaining molecular insight into immune reactions could so far not be exploited due to the lack of gene editing

Figure 5. CRISPR-Cas9-mediated gene editing of tonsil CD4 T cells can be used as a tool to mechanistically dissect T cell activation and CD4 T cell helper function

(A) Schematic of the experimental setup to assess activation response of CD4 T cells after nucleofection of bulk or isolated CD4 T cells. Briefly, bulk cells or positively isolated CD4 T cells after bead removal were either left untreated or nucleofected with NT RNP complex prior to seeding, i.e., merging with non-CD4 T cells for the reconstituted culture. One day after seeding, cultures were stimulated with SEB or left untreated and activation response was assessed on subsequent days by flow cytometry.

(B and C) Representative histograms showing CD69, CD25, CD38, and HLA-DR expression on tonsil CD4 T cells on day 7 post nucleofection of bulk cells (B) or isolated CD4 T cells (C). Superimposed histograms show expression profiles of the non-nucleofected culture (gray) and cultures nucleofected with non-targeting control (NT Ctrl) RNP (red). Dashed lines represent unstimulated conditions while solid lines represent SEB-stimulated cultures.

(D and E) Quantification of (B) and (C) for day 1, day 8, and day 13 post SEB stimulation for non-nucleofected or NT conditions with and without stimulation after bulk (D) or isolated CD4 T cell (E) nucleofection. Each symbol represents one donor. Shown are means with SD. Tonsil cells were cultured in 96-well F-bottom plates.

(F) Schematic of the experimental setup for assessing immunocompetency of tonsil bulk or CD4 T cells after nucleofection. Briefly, bulk cells or positive isolated CD4 T cells after bead removal were either left untreated or nucleofected with NT RNP complex prior to seeding, i.e., merging with non-CD4 T cells for the reconstituted culture. Seven days after seeding, EBV peptide pool was added together with interleukin (IL)-7. On day 7 and day 14, baseline and expanded EBV-specific CD8 T cells, respectively, were identified by production of IFNγ following stimulation with the EBV peptide pool.

(G) Representative dot plots showing IFNγ+ CD8 T cells in tonsil cultures for bulk or isolated CD4 T cell nucleofection (NT Ctrl.) in comparison with untreated (no nucl.) conditions on day 7 or day 14 of culture upon restimulation with EBV PP, respectively.

(H and I) Quantification of (G) for five tonsils, showing frequency of IFNγ+ CD8 T cells on day 14 in cultures were either bulk cells or isolated CD4 T cells were left untreated (no nucl) or nucleofected with NT Ctrl. Shown are means with SD. Each symbol represents one donor.

(J and M) Characterization of memory subsets based on expression of CD45RO and CD62L among total CD8 (J) or CD4 (M) T cells (gray) or superimposed IFNγ+ CD8 T cells (J) (red) on day 14 following peptide stimulation of tonsil cells cultured with EBV peptide pool for 7 days (K) and (L). Quantification of (J) for total CD8 T cells in cultures where bulk cells (left) or isolated CD4 T cells (right) were nucleofected (NT Ctrl.) or left untreated (no nucl.).

(N and O) Quantification of (M) as described above. T_{Eff} = T effector cells, T_{EM} = effector memory cells, T_{CM} = central memory cells, T_{naive} = naive T cells. Shown are means with SD for five tonsils. Tonsil cells were cultured in 96-well F-bottom plates. Statistical significance was assessed by repeated-measures one-way ANOVA for data in (D) and (E), except for CD38 expression after bulk nucleofection and HLA-DR expression after CD4 nucleofection where data were not normally distributed and Friedman test was used instead. For (H) and (I), Friedman test was used for comparison of more than two groups and Wilcoxon test was used for data in (K), (L), (N), and (O) for comparison of two groups, ns, $p > 0.05$; *$p < 0.05$; **$p < 0.01$; ***$p < 0.001$; ****$p < 0.0001$.

methods that allow for modification of gene expression with high precision and without impairing the activation state and immune competence of tonsil-resident cells. In the case of HLAC, a particular challenge for such an approach lies in the fact that close to 100% KO efficiency is required to conduct meaningful studies, since even minor contamination with unedited subpopulations may be sufficient to exert complex functions, expand in the course of the experiment, and thereby potentially mislead conclusion on the relevance of the gene of interest in the process studied. Furthermore, the gene editing approach per se should not affect the intrinsic properties of the edited cells. The ediTONSIL workflow established herein offers these possibilities as it allows gene editing with over 90% efficacy without requiring exogenous activation. Editing can in principle be done in bulk cultures to effectively target all major cell populations in parallel, although this comes at the cost of a significantly reduced cell viability. However, because HLACs are launched as suspension cultures that subsequently reorganize into immune-competent structures, specific cell populations can be isolated and edited at the beginning of an experiment and embedded in their natural cellular environment immediately after editing. Importantly, several lines of evidence document that ediTONSIL does not alter the tissue-resident characteristics of the edited tonsillar CD4 T cells: upon reintroduction into their natural cell environment they (1) are permissive to productive HIV infection without exogenous stimulation, (2) respond to TCR stimulation, and (3) exert helper function for CD8 T cell responses. ediTONSIL of isolated CD4 T cells with subsequent reconstitution of the culture therefore neither cause cell activation per se nor does it impair the activation response to external stimulation such as antigenic stimulation of CD4 T cells and also preserves the competence for complex functional cell-cell interaction such as CD4 T cell help to a recall CD8 T cell response. As illustrated at the example of HIV-1 infection, kinetics and magnitude of virus replication as well as CD4 T cell depletion are unaffected by the editing approach but targeting essential host cell genes such as the entry co-receptor fully abrogates virus infection and spread. Moreover, dye labeling of edited cells prior to reintegration in the complex organotypic cultures provides a convenient tool to identify and visualize them over extended periods of time in their natural cell environment. Adapting the methodology established here for tonsillar CD4 T cells to, e.g., CD8 T cells, B cells, and myeloid cells will offer a versatile toolbox to study mechanisms in all cell types present in the culture. This allows precise dissection of molecular mechanisms in basic immunology but also complex cell-cell interactions in the tissue context. This may be instrumental for, e.g., dissecting the mechanisms underlying CD4 T cell help to CD8 T cell responses, which is an emerging concept in infectious diseases and cancer[44–47] and insights yielded from ediTONSIL studies in a human lymphoid tissue system will complement *in vivo* mouse studies. Importantly, this culture system is also suitable to study humoral immunity, e.g., B cell antibody production to recall antigens but also *de novo* vaccine responses and ediTONSIL opens further possibilities to study B cell responses.[7,19,20] Furthermore, studies on viral pathogenesis and cell interactions in *ex vivo* tonsil cultures, exemplified herein with HIV-1, can be expanded to other pathogen infections including HTLV, human herpesviruses (HHV-6, HHV-7, HCMV, HSV-2, EBV), vaccinia virus, measles virus, and West-Nile virus.[17,40–43,48–53] ediTONSIL thus opens avenues toward the mechanistic dissection in organotypic lymphoid cultures and will be widely applied to studies of pathogen-host interaction but also of fundamental principles of adaptive immunity.

Limitations of the study

The workflow developed herein allows for the efficient gene editing of bulk or individual cell populations in *ex vivo* tonsil cultures. For individual cell populations, however, the isolation efficiency is a critical parameter and the success of ediTONSIL depends on the availability and quality of commercial or in-house isolation procedures for cells of interest. Furthermore, it is important to note that the half-life of each individual target protein is a key determinant. Since the viability of these *ex vivo* cultures significantly decreases after 2 weeks, proteins with low turnover will not be sufficiently depleted within the lifespan of the culture. The fact that the applicability of this workflow depends on these individual features of each target implies that KOs must be monitored specifically for each target, which currently precludes the use of this method for high-throughput screening approaches. Establishing conditions that expand the lifespan of these model cultures will be a central goal of future developments.

STAR★METHODS

Detailed methods are provided in the online version of this paper and include the following:

- KEY RESOURCES TABLE
- RESOURCE AVAILABILITY
  - Lead contact
  - Materials availability
  - Data and code availability
- EXPERIMENTAL MODEL AND STUDY PARTICIPANT DETAILS
  - Human lymphoid aggregate culture (HLAC)
  - Cell culture
- METHOD DETAILS
  - Virus production, infectivity measurements, infection assays, and CD4 T cell depletion
  - Flow cytometry analysis
  - Quantification of HIV-1 induced CD4 T cell depletion
  - RNP preparation
  - CRISPR/Cas9 RNP nucleofection of tonsil cells
  - SEB stimulation of tonsil cell cultures
  - Cytokine treatment of tonsil cell cultures for optimization of post-nucleofection conditions
  - T20 treatment of tonsil cells to inhibit fusion and entry of HIV-1
  - CD4 positive and negative isolation from tonsil cell suspension
  - Celltracker staining of isolated tonsil CD4 T cells
  - Reactivation and expansion of EBV-specific memory CD8 T cells in tonsil tissue
- QUANTIFICATION AND STATISTICAL ANALYSIS

SUPPLEMENTAL INFORMATION

Supplemental information can be found online at https://doi.org/10.1016/j.crmeth.2023.100685.

ACKNOWLEDGMENTS

This project is supported by the Deutsche Forschungsgemeinschaft (DFG, German Research Foundation), Projektnummer 240245660 - SFB 1129 (project 8) and Projektnummer 259021520 – FA 378/13-2, OK 742/5-2) and the German Center for Infection Research (DZIF) (TTU 04.820 – HIV reservoir to O.T.F., O.T.K.). O.T.F. is a member of the CellNetworks cluster of excellence (EXC81). We want to especially thank Nadine Tibroni, Ina Ambiel, and the Head and Neck Surgery team for support with the acquisition of tonsil specimens and all anonymous tonsil donors that made this study possible.

AUTHOR CONTRIBUTIONS

Conceptualization, O.T.F.; Methodology, L.S. and O.T.K.; Investigation, K.M.; Visualization: K.M.; Writing – Original Draft, O.T.F. and K.M.; Writing –Review & Editing, O.T.F, K.M., G.D., and O.T.K; Funding Acquisition, O.T.F., O.T.K.; Resources, D.G.; Supervision, O.T.F.; Project administration: O.T.F.

DECLARATION OF INTERESTS

The authors declare no competing interests.

Received: August 18, 2023
Revised: November 13, 2023
Accepted: December 13, 2023
Published: January 10, 2024

REFERENCES

1. Swain, S.L., McKinstry, K.K., and Strutt, T.M. (2012). Expanding roles for CD4⁺ T cells in immunity to viruses. Nat. Rev. Immunol. *12*, 136–148.
2. Medetgul-Ernar, K., and Davis, M.M. (2022). Standing on the shoulders of mice. Immunity *55*, 1343–1353.
3. Zhang, C., Zaman, L.A., Poluektova, L.Y., Gorantla, S., Gendelman, H.E., and Dash, P.K. (2023). Humanized mice for studies of HIV-1 persistence and elimination. Pathogens *12*.
4. Marsden, M.D. (2020). Benefits and limitations of humanized mice in HIV persistence studies. Retrovirology *17*, 7.
5. Glushakova, S., Baibakov, B., Margolis, L.B., and Zimmerberg, J. (1995). Infection of human tonsil histocultures: a model for HIV pathogenesis. Nature Medicine *1*, 1320–1322.
6. Glushakova, S., Baibakov, B., Zimmerberg, J., and Margolis, L.B. (1997). Experimental HIV infection of human lymphoid tissue: correlation of CD4+ T cell depletion and virus syncytium-inducing/non-syncytium-inducing phenotype in histocultures inoculated with laboratory strains and patient isolates of HIV type 1. AIDS Res. Hum. Retrovir. *13*, 461–471.
7. Glushakova, S., Grivel, J.C., Fitzgerald, W., Sylwester, A., Zimmerberg, J., and Margolis, L.B. (1998). Evidence for the HIV-1 phenotype switch as a causal factor in acquired immunodeficiency. Nature Medicine *4*, 346–349.
8. Margolis, L.B., Glushakova, S., Grivel, J.C., and Murphy, P.M. (1998). Blockade of CC chemokine receptor 5 (CCR5)-tropic human immunodeficiency virus-1 replication in human lymphoid tissue by CC chemokines. J. Clin. Invest. *101*, 1876–1880.
9. Eckstein, D.A., Penn, M.L., Korin, Y.D., Scripture-Adams, D.D., Zack, J.A., Kreisberg, J.F., Roederer, M., Sherman, M.P., Chin, P.S., and Goldsmith, M.A. (2001). HIV-1 actively replicates in naive CD4(+) T cells residing within human lymphoid tissues. Immunity *15*, 671–682.
10. Reif, T., Dyckhoff, G., Hohenberger, R., Kolbe, C.C., Gruell, H., Klein, F., Latz, E., Stolp, B., and Fackler, O.T. (2021). Contact-dependent inhibition of HIV-1 replication in ex vivo human tonsil cultures by polymorphonuclear neutrophils. Cell Rep. Med. *2*, 100317.
11. Penn, M.L., Grivel, J.C., Schramm, B., Goldsmith, M.A., and Margolis, L. (1999). CXCR4 utilization is sufficient to trigger CD4+ T cell depletion in HIV-1-infected human lymphoid tissue. Proc Natl Acad Sci USA *96*, 663–668.
12. Jayakumar, P., Berger, I., Autschbach, F., Weinstein, M., Funke, B., Verdin, E., Goldsmith, M.A., and Keppler, O.T. (2005). Tissue-resident macrophages are productively infected ex vivo by primary X4 isolates of human immunodeficiency virus type 1. J. Virol. *79*, 5220–5226.
13. Homann, S., Tibroni, N., Baumann, I., Sertel, S., Keppler, O.T., and Fackler, O.T. (2009). Determinants in HIV-1 Nef for enhancement of virus replication and depletion of CD4+ T lymphocytes in human lymphoid tissue ex vivo. Retrovirology *6*, 6.
14. Muñoz-Arias, I., Doitsh, G., Yang, Z., Sowinski, S., Ruelas, D., and Greene, W.C. (2015). Blood-Derived CD4 T Cells Naturally Resist Pyroptosis during Abortive HIV-1 Infection. Cell Host Microbe *18*, 463–470.
15. Audigé, A., Urosevic, M., Schlaepfer, E., Walker, R., Powell, D., Hallenberger, S., Joller, H., Simon, H.U., Dummer, R., and Speck, R.F. (2006). Anti-HIV state but not apoptosis depends on IFN signature in CD4+ T cells. JJ. Immunol. *177*, 6227–6237.
16. Doitsh, G., Galloway, N.L.K., Geng, X., Yang, Z., Monroe, K.M., Zepeda, O., Hunt, P.W., Hatano, H., Sowinski, S., Muñoz-Arias, I., and Greene, W.C. (2014). Cell death by pyroptosis drives CD4 T-cell depletion in HIV-1 infection. Nature *505*, 509–514.
17. Grivel, J.C., and Margolis, L. (2009). Use of human tissue explants to study human infectious agents. Nat. Protoc. *4*, 256–269.
18. Kaw, S., Ananth, S., Tsopoulidis, N., Morath, K., Coban, B.M., Hohenberger, R., Bulut, O.C., Klein, F., Stolp, B., and Fackler, O.T. (2020). HIV-1 infection of CD4 T cells impairs antigen-specific B cell function. Embo j *39*, e105594.
19. Wagar, L.E., Salahudeen, A., Constantz, C.M., Wendel, B.S., Lyons, M.M., Mallajosyula, V., Jatt, L.P., Adamska, J.Z., Blum, L.K., Gupta, N., et al. (2021). Modeling human adaptive immune responses with tonsil organoids. Nature medicine *27*, 125–135.
20. Kastenschmidt, J.M., Sureshchandra, S., Jain, A., Hernandez-Davies, J.E., de Assis, R., Wagoner, Z.W., Sorn, A.M., Mitul, M.T., Benchorin, A.I., Levendosky, E., et al. (2023). Influenza vaccine format mediates distinct cellular and antibody responses in human immune organoids. Immunity *56*, 1910–1926.e7.
21. Albanese, M., Ruhle, A., Mittermaier, J., Mejías-Pérez, E., Gapp, M., Linder, A., Schmacke, N.A., Hofmann, K., Hennrich, A.A., Levy, D.N., et al. (2022). Rapid, efficient and activation-neutral gene editing of polyclonal primary human resting CD4(+) T cells allows complex functional analyses. Nat. Methods *19*, 81–89.
22. Packard, T.A., Schwarzer, R., Herzig, E., Rao, D., Luo, X., Egedal, J.H., Hsiao, F., Widera, M., Hultquist, J.F., Grimmett, Z.W., et al. (2022). CCL2: a Chemokine Potentially Promoting Early Seeding of the Latent HIV Reservoir. mBio *13*, e0189122.
23. Hultquist, J.F., Schumann, K., Woo, J.M., Manganaro, L., McGregor, M.J., Doudna, J., Simon, V., Krogan, N.J., and Marson, A. (2016). A Cas9 Ribonucleoprotein Platform for Functional Genetic Studies of HIV-Host Interactions in Primary Human T Cells. Cell Rep. *17*, 1438–1452.
24. Schmidt, A., Huber, J.E., Sercan Alp, Ö., Gürkov, R., Reichel, C.A., Herrmann, M., Keppler, O.T., Leeuw, T., and Baumjohann, D. (2020). Complex human adenoid tissue-based ex vivo culture systems reveal anti-inflammatory drug effects on germinal center T and B cells. EBioMedicine *53*, 102684.
25. Masur, H., Michelis, M.A., Greene, J.B., Onorato, I., Stouwe, R.A., Holzman, R.S., Wormser, G., Brettman, L., Lange, M., Murray, H.W., and Cunningham-Rundles, S. (1981). An outbreak of community-acquired Pneumocystis carinii pneumonia: initial manifestation of cellular immune dysfunction. N. Engl. J. Med. *305*, 1431–1438.

26. Gottlieb, M.S., Schroff, R., Schanker, H.M., Weisman, J.D., Fan, P.T., Wolf, R.A., and Saxon, A. (1981). Pneumocystis carinii pneumonia and mucosal candidiasis in previously healthy homosexual men: evidence of a new acquired cellular immunodeficiency. N. Engl. J. Med. *305*, 1425–1431.

27. Pizzato, M., Erlwein, O., Bonsall, D., Kaye, S., Muir, D., and McClure, M.O. (2009). A one-step SYBR Green I-based product-enhanced reverse transcriptase assay for the quantitation of retroviruses in cell culture supernatants. J. Virol. Methods *156*, 1–7.

28. Ananth, S., Morath, K., Trautz, B., Tibroni, N., Shytaj, I.L., Obermaier, B., Stolp, B., Lusic, M., and Fackler, O.T. (2019). Multi-functional roles of the N-terminal region of HIV-1SF2Nef are mediated by three independent protein interaction sites. J. Virol. *94*. e01398-19.

29. Janssen, E.M., Lemmens, E.E., Wolfe, T., Christen, U., von Herrath, M.G., and Schoenberger, S.P. (2003). CD4+ T cells are required for secondary expansion and memory in CD8+ T lymphocytes. Nature *421*, 852–856.

30. Shedlock, D.J., and Shen, H. (2003). Requirement for CD4 T cell help in generating functional CD8 T cell memory. Science *300*, 337–339.

31. Eickhoff, S., Brewitz, A., Gerner, M.Y., Klauschen, F., Komander, K., Hemmi, H., Garbi, N., Kaisho, T., Germain, R.N., and Kastenmüller, W. (2015). Robust Anti-viral Immunity Requires Multiple Distinct T Cell-Dendritic Cell Interactions. Cell *162*, 1322–1337.

32. Hor, J.L., Whitney, P.G., Zaid, A., Brooks, A.G., Heath, W.R., and Mueller, S.N. (2015). Spatiotemporally Distinct Interactions with Dendritic Cell Subsets Facilitates CD4+ and CD8+ T Cell Activation to Localized Viral Infection. Immunity *43*, 554–565.

33. Long, H.M., Meckiff, B.J., and Taylor, G.S. (2019). The T-cell Response to Epstein-Barr Virus-New Tricks From an Old Dog. Front. Immunol. *10*, 2193.

34. Hislop, A.D., Kuo, M., Drake-Lee, A.B., Akbar, A.N., Bergler, W., Hammerschmitt, N., Khan, N., Palendira, U., Leese, A.M., Timms, J.M., et al. (2005). Tonsillar homing of Epstein-Barr virus-specific CD8+ T cells and the virus-host balance. J. Clin. Invest. *115*, 2546–2555.

35. Chaganti, S., Heath, E.M., Bergler, W., Kuo, M., Buettner, M., Niedobitek, G., Rickinson, A.B., and Bell, A.I. (2009). Epstein-Barr virus colonization of tonsillar and peripheral blood B-cell subsets in primary infection and persistence. Blood *113*, 6372–6381.

36. Moutsopoulos, N.M., Vázquez, N., Greenwell-Wild, T., Ecevit, I., Horn, J., Orenstein, J., and Wahl, S.M. (2006). Regulation of the tonsil cytokine milieu favors HIV susceptibility. J. Leukoc. Biol. *80*, 1145–1155.

37. Kreisberg, J.F., Yonemoto, W., and Greene, W.C. (2006). Endogenous factors enhance HIV infection of tissue naive CD4 T cells by stimulating high molecular mass APOBEC3G complex formation. JJ. Exp. Med. *203*, 865–870.

38. Demirci, S., Haro-Mora, J.J., Leonard, A., Drysdale, C., Malide, D., Keyvanfar, K., Essawi, K., Vizcardo, R., Tamaoki, N., Restifo, N.P., et al. (2020). Definitive hematopoietic stem/progenitor cells from human embryonic stem cells through serum/feeder-free organoid-induced differentiation. Stem Cell Res. Ther. *11*, 493.

39. Rao, I., Crisafulli, L., Paulis, M., and Ficara, F. (2022). Hematopoietic Cells from Pluripotent Stem Cells: Hope and Promise for the Treatment of Inherited Blood Disorders. Cells *11*.

40. Lisco, A., Vanpouille, C., Tchesnokov, E.P., Grivel, J.C., Biancotto, A., Brichacek, B., Elliott, J., Fromentin, E., Shattock, R., Anton, P., et al. (2008). Acyclovir is activated into a HIV-1 reverse transcriptase inhibitor in herpesvirus-infected human tissues. Cell Host Microbe *4*, 260–270.

41. Langlois, M., Bounou, S., Tremblay, M.J., and Barbeau, B. (2023). Infection of the Ex Vivo Tonsil Model by HTLV-1 Envelope-Pseudotyped Viruses. Pathogens *12*, 182.

42. Pegtel, D.M., Middeldorp, J., and Thorley-Lawson, D.A. (2004). Epstein-Barr virus infection in ex vivo tonsil epithelial cell cultures of asymptomatic carriers. J. Virol. *78*, 12613–12624.

43. Grivel, J.C., Santoro, F., Chen, S., Fagá, G., Malnati, M.S., Ito, Y., Margolis, L., and Lusso, P. (2003). Pathogenic effects of human herpesvirus 6 in human lymphoid tissue ex vivo. J. Virol. *77*, 8280–8289.

44. Lu, Y.J., Barreira-Silva, P., Boyce, S., Powers, J., Cavallo, K., and Behar, S.M. (2021). CD4 T cell help prevents CD8 T cell exhaustion and promotes control of Mycobacterium tuberculosis infection. Cell Rep. *36*, 109696.

45. Ferris, S.T., Durai, V., Wu, R., Theisen, D.J., Ward, J.P., Bern, M.D., Davidson, J.T., 4th, Bagadia, P., Liu, T., Briseño, C.G., et al. (2020). cDC1 prime and are licensed by CD4(+) T cells to induce anti-tumour immunity. Nature *584*, 624–629.

46. Borst, J., Ahrends, T., Bąbała, N., Melief, C.J.M., and Kastenmüller, W. (2018). CD4(+) T cell help in cancer immunology and immunotherapy. Nat. Rev. Immunol. *18*, 635–647.

47. Zander, R., Schauder, D., Xin, G., Nguyen, C., Wu, X., Zajac, A., and Cui, W. (2019). CD4(+) T Cell Help Is Required for the Formation of a Cytolytic CD8(+) T Cell Subset that Protects against Chronic Infection and Cancer. Immunity *51*, 1028–1042.e4.

48. Grivel, J.C., Ito, Y., Faga, G., Santoro, F., Shaheen, F., Malnati, M.S., Fitzgerald, W., Lusso, P., and Margolis, L. (2001). Suppression of CCR5- but not CXCR4-tropic HIV-1 in lymphoid tissue by human herpesvirus 6. Nature Medicine *7*, 1232–1235.

49. Lisco, A., Grivel, J.C., Biancotto, A., Vanpouille, C., Origgi, F., Malnati, M.S., Schols, D., Lusso, P., and Margolis, L.B. (2007). Viral interactions in human lymphoid tissue: Human herpesvirus 7 suppresses the replication of CCR5-tropic human immunodeficiency virus type 1 via CD4 modulation. J. Virol. *81*, 708–717.

50. Biancotto, A., Iglehart, S.J., Lisco, A., Vanpouille, C., Grivel, J.C., Lurain, N.S., Reichelderfer, P.S., and Margolis, L.B. (2008). Upregulation of human cytomegalovirus by HIV type 1 in human lymphoid tissue ex vivo. AIDS Res. Hum. Retrovir. *24*, 453–462.

51. Vanpouille, C., Biancotto, A., Lisco, A., and Brichacek, B. (2007). Interactions between human immunodeficiency virus type 1 and vaccinia virus in human lymphoid tissue ex vivo. J. Virol. *81*, 12458–12464.

52. Condack, C., Grivel, J.C., Devaux, P., Margolis, L., and Cattaneo, R. (2007). Measles virus vaccine attenuation: suboptimal infection of lymphatic tissue and tropism alteration. J. Infect. Dis. *196*, 541–549.

53. Lim, J.K., Lisco, A., McDermott, D.H., Huynh, L., Ward, J.M., Johnson, B., Johnson, H., Pape, J., Foster, G.A., Krysztof, D., et al. (2009). Genetic variation in OAS1 is a risk factor for initial infection with West Nile virus in man. PLoS Pathog. *5*, e1000321.

54. Fackler, O.T., Moris, A., Tibroni, N., Giese, S.I., Glass, B., Schwartz, O., and Krausslich, H.G. (2006). Functional characterization of HIV-1 Nef mutants in the context of viral infection. Virology *351*, 322–339.

55. Pear, W.S., Nolan, G.P., Scott, M.L., and Baltimore, D. (1993). Production of high-titer helper-free retroviruses by transient transfection. Proc. Natl. Acad. Sci. USA *90*, 8392–8396.

56. Platt, E.J., Wehrly, K., Kuhmann, S.E., Chesebro, B., and Kabat, D. (1998). Effects of CCR5 and CD4 cell surface concentrations on infections by macrophagetropic isolates of human immunodeficiency virus type 1. J. Virol. *72*, 2855–2864.

57. Vermeire, J., Naessens, E., Vanderstraeten, H., Landi, A., Iannucci, V., Van Nuffel, A., Taghon, T., Pizzato, M., and Verhasselt, B. (2012). Quantification of reverse transcriptase activity by real-time PCR as a fast and accurate method for titration of HIV, lenti- and retroviral vectors. PLoS One *7*, e50859.

STAR★METHODS

KEY RESOURCES TABLE

REAGENT or RESOURCE	SOURCE	IDENTIFIER
Antibodies		
CD3-PE (clone SK7)	BD Biosciences	Cat#345765; RRID:AB_2868796
CD3-PerCP (clone SK7)	Biolegend	Cat#344814; RRID:AB_10639948
CD3-BV785 (clone UCHT1)	Biolegend	Cat#300472; RRID:AB_2687178
CD4-BV421 (clone RPA-T4)	BD Biosciences	Cat#562424; RRID:AB_11154417
CD4-A647 (clone OKT4)	Biolegend	Cat#317422; RRID:AB_571941
CD8-FITC (clone SK1)	Biolegend	Cat#344703; RRID:AB_1877178
CD8-APC (clone SK1)	Biolegend	Cat#344722; RRID:AB_2075390
CD8-PerCP (clone SK1)	Biolegend	Cat#344708; RRID:AB_1967122
CD19-PE (clone HIB19)	Biolegend	Cat#302207; RRID:AB_314238
CD45-APC-Cy7 (clone 2D1)	Biolegend	Cat#368515; RRID:AB_2566376
HLA-DR-BV510 (clone L243)	Biolegend	Cat#307646; RRID:AB_2561396
CD38-A488 (clone HIT2)	Biolegend	Cat#303512; RRID:AB_493088
CD25-PE (clone M-A251)	Biolegend	Cat#356103; RRID:AB_2564145
CD69-APC-Cy7 (clone FN50)	Biolegend	Cat#310914; RRID:AB_314849
CD11c-BV605 (clone 3.9)	Biolegend	Cat#301636; RRID:AB_2563796
CD11b-A488 (clone ICRF44)	Biolegend	Cat#301318; RRID:AB_493017
CD45RA-FITC (clone MEM-56)	Immunotools	Cat#21279453
CD45RO-PE (clone UCHL1)	Biolegend	Cat#304205; RRID:AB_2564160
CD62L-BV510 (clone DREG-56)	Biolegend	Cat#304843; RRID:AB_2617003
CXCR4-PE (clone 12G5)	Biolegend	Cat#306506; RRID:AB_314611
CXCR4-APC (clone 12G5)	Biolegend	Cat#306510; RRID:AB_314616
P24-FITC (clone KC57)	Beckman Coulter	Cat#6604665; RRID:AB_1575987
IFNγ-FITC (clone 4S.B3)	Biolegend	Cat#502507; RRID:AB_315230
Bacterial and virus strains		
HIV-1 NL4.3 $SF2_{nef}$	Fackler et al. (2006)[54]	N/A
Biological samples		
Human tonsil tissue	Department of Otorhinolaryngology, Head and Neck Surgery, University Hospital Heidelberg, Germany	N/A
Chemicals, peptides, and recombinant proteins		
PepTivator® EBV Consensus – premium grade	Miltenyi Biotec	Cat#130-103-462
HIV-1 Gag epitope pool	NIH AIDS Reagent Program	Cat#ARP-12437
HIV-1 Env epitope pool	NIH AIDS Reagent Program	Cat#ARP-12698
ITS-G (Insulin-Transferrin-Selen) Cocktail 100x	Thermo Fisher Scientific	Cat#41400045
FBS, heat-inactivated	Capricorn	Cat#FBS-HI-12A
RPMI 1640	Gibco/Thermo Fisher Scientific	Cat#61870036
Non-essential amino acids 100x	Gibco/Thermo Fisher Scientific	Cat#11140050
Amphotericin B/Fungizone 100x	Gibco/Thermo Fisher Scientific	Cat#15290026
Penicillin/Streptomycin Solution 100x	Capricorn	Cat#PS-B
DMEM, high glucose	GlutaMAX™ Supplement	Cat#61965026
Ficoll® Paque Plus	Merck	Cat#GE17144003
T20/Fuzeon/Enfuvirtide	Roche	N/A
DeepRed celltracker dye	Thermo Fisher Scientific	Cat#C34565

(*Continued on next page*)

Continued

REAGENT or RESOURCE	SOURCE	IDENTIFIER
Zombie violet fixable viability kit	Biolegend	Cat#423113
Brefeldin A	Sigma	Cat#B6542
IL-7	Biolegend	Cat#581902
IL-15	Biolegend	Cat#570302
IL-2	Biomol	Cat#50442
Critical commercial assays		
BD Cytofix/Cytoperm kit	BD Biosciences	Cat#554714
EasySep™ Release Human CD4 Positive Selection Kit	Stemcell Technologies	Cat#17752
EasySep™ Human CD4+ T cell Isolation Kit	Stemcell Technologies	Cat#17952
Experimental models: Cell lines		
Human embryonic kidney 293 T cells (HEK293T)	Pear et al. (1993)[55]	RRID:CVCL_1926; ATCC Cat#CRL-11268
TZM-bl cells, human carcinoma cell, derived from HeLa	NIH AIDS Reagents Program (Platt et al., 1998)[56]	PRID: CVCL_B478; Cat#8129-442
Oligonucleotides		
SG-PERT fwd primer; TCCTGCTCAA CTTCCTGTCGAG	Vermeire et al. (2012)[57]	N/A
SG-PERT rev primer; CACAGGTCAA ACCTCCTAGGAATG	Vermeire et al. (2012)[57]	N/A
CXCR4 sgRNA1	Albanese et al. (2021)[21]	N/A
CXCR4 sgRNA2	Albanese et al. (2021)[21]	N/A
Recombinant DNA		
pHIV-1NL4.3 SF2 Nef X4	Fackler et al. (2006)[54]	N/A
Software and algorithms		
BD FACSDiva Software	BD Biosciences	www.bdbiosciences.com
BD FACSuite Software	BD Biosciences	www.bdbiosciences.com
FlowJo software 10.4.2	BD Biosciences	www.flowjo.com
Microsoft Office Excel 2016	Microsoft Office	www.microsoft.com
Prism 8.0.1	GraphPad	www.graphpad.com
Other		
Stemcell EasySep Magnet	Stemcell technologies	Cat#18000
100 μm PET cell strainer	PluriSelect Life Science	Cat#43-50100-51
24-Well Insert PET	cellQART	Cat#932 04 02

RESOURCE AVAILABILITY

Lead contact

Further information and requests for resources and reagents should be directed to and will be fulfilled by the Lead Contact, Prof. Dr. Oliver T. Fackler (oliver.fackler@med.uni-heidelberg.de).

Materials availability

This study did not generate new unique reagents.

Data and code availability

(1) All primary data generated in this study are available from the lead contact upon request. The flow cytometry datasets will be publicly available on FlowRepository when sufficient storage capacity is available.
(2) This Paper does not report original code
(3) Any additional information required to reanalyze the data reported in this paper is available from the lead contact upon request.

EXPERIMENTAL MODEL AND STUDY PARTICIPANT DETAILS

Human lymphoid aggregate culture (HLAC)

HLACs were generated as previously described.[19] Tonsils were removed and received from randomly selected anonymous donors with informed consent in accordance with the ethics vote S-123/2014 from the Heidelberg University Hospital ethics committee. Gender and age of the donors is not known. One-half of each tonsil was collected during standard tonsillectomy while the other half was processed in the department of pathology to assess chronic tonsillitis and exclude any unexpected malignancy. Removed tonsil tissue was immediately transferred to 50mL Falcon tubes containing 1X phosphate-buffered saline (PBS) and processed on the same day as described.[19] In brief, dead and burnt tissue was removed and tonsils were sliced into blocks of approximately 2mm size that were passed through a 100 μm mash PET strainer. The suspension was filled up with PBS to 35 mL and erythrocytes and debris was removed from the cell suspension by layering onto 15 mL of Ficoll Separating Solution and centrifugation for 20 min at 2000 rpm (Heraeus MEGAFUGE 40R) without break at room temperature. The mononuclear fraction above the erythrocyte layer was isolated, washed twice with PBS and frozen in 90% FBS with 10% DMSO at −80°C in aliquots of $1x10^8$ cells/ml. For experiments, cells were thawed in tonsil medium (RPMI 1640 GlutaMAX, 10% FCS, 5% Fungizone, 5% non-essential amino acids, 5% Sodium Pyruvate, 5% Penicillin/Streptomycin, 5% ITS-G), washed twice and resuspended in 10 mL medium prior to viability and cell counting in a 1:100 dilution with Trypan blue. Cells were resuspended in tonsil medium at $1x10^7$ cells/ml and 200 μL of the cell suspension was added per well of a V or F-bottom 96-well plate. For transwell culture in 24-well plates, cells were resuspended at $4x10^7$ cells/ml and 50μL cell suspension was added to the upper transwell while the lower well was filled with 500 μL medium. Transwells were equilibrated with medium prior to use. Cells were cultured at 37°C, 5% CO_2 under humidified conditions for up to three weeks.

Cell culture

Human embryonic kidney 293T (HEK293T) cells were cultured in Dulbecco's modified Eagle medium (DMEM; ThermoFisher Scientific) containing 10% FCS, 5% penicillin and 5% streptomycin. The cells are female and have not been authenticated.

TZM-bl cells (JC53BL-13) were obtained from the NIH AIDS Research and Reference Reagent Program (Cat. no. 8129) and are derived from a HeLa cell clone that was engineered to express CD4, CCR5 and CXCR4 to allow entry of X4-and R5-tropic HIV-1 strains[56] and further contains integrated reporter genes for firefly Luc and *E. coli* β-galactosidase under the control of an HIV-1 long terminal repeat. For determination of virus stock infectivity, TZM-bl cells were infected with titrated amounts of the virus and X-β-Gal substrate was added after 2–3 days. The substrate is converted by the β-galactosidase to a blue colored product that is used to assess infection of TZM-bl cells and relative infectivity of the virus stock.

METHOD DETAILS

Virus production, infectivity measurements, infection assays, and CD4 T cell depletion

Virus production from 293T cells, infectivity measurements using SG-PERT for total viral particles and TZM-bl reporter assay were performed as described previously.[27,28] $2x10^6$ tonsil cells were infected with $1.5x10^5$ BCU/well of the CXCR4 tropic chimera HIV-1NL4.3 $SF2_{nef}$ (X4-tropic HIV-1)[54]. For F- and V-bottom 96-well plates, virus was diluted in 100 μL/well and added after removal of 100 μL spent medium from each well. For transwell plates, 250μL medium were removed from the lower transwell and virus was added in 250μL fresh medium. Mock wells were treated accordingly without addition of virus to the medium. One day post-infection (dpi) HLACs were washed 3x with 200 μL tonsil medium for V- and F-bottom 96-well plates by centrifugation at 1200 rpm for 5 min at RT and addition of fresh medium after washing. Transwell cultures were washed by 3x renewal of the lower transwell medium (500 μL) with 1 min incubation time respectively to allow full submerging of the upper transwell and transition of input virus in the supernatant to the lower well. HLACs were cultured for 7–15 days post infection. Every two to three days, 5 μL supernatant for determination of viral titers was harvested. The measurement started 1 dpi with the initial supernatant collected after the washing step.

Flow cytometry analysis

Tonsil cells were washed with PBS and stained with zombie violet fixable viability dye (1:1000 in PBS), incubated for 15 min at RT and washed with FACS buffer (1xPBS +0.5% BSA +2mM EDTA) prior to surface antibody staining. Surface staining of CD45, CD3, CD4, CD8, CD19, HLA-DR, CD11b, CD11c, CD38, CD25, CD69, CD45RO, CD45RA, CD62L and CXCR4 was performed at a 1:100 dilution of antibodies in FACS buffer and incubation at 4°C for 20 min, respectively. Cells were then washed and fixed with 3% PFA for 10 min or 90 min for BSL-3 sample inactivation. For intracellular staining of HIV-1 capsid (p24), cells were then resuspended in 0.1% Triton X-100 containing 1:100 diluted anti-p24 antibody (clone KC57, Beckman Coulter) and incubated for 20 min at 4°C and acquired on the same day. For intracellular staining of IFNγ, cells after surface staining and PFA fixation were permeabilized and stained using the BD Cytofix/Cytoperm kit according to the manufacturer's protocol. Briefly, cells were incubated in Cytofix/Cytoperm solution for 20 min at 4°, washed 2x with 1xPerm buffer and resuspended in 1xPerm buffer containing 1:100 diluted anti-human IFNγ antibody. Samples were incubated for 30 min at 4°C, washed and acquired by flow cytometry on the same day.

Samples were acquired using a BD FACSVerse with BD FACSuite Software or FACS Celesta with BD FACS Diva software. Gating was performed using FlowJo software 10.4.2 and data was processed with Microsoft Office Excel 2016 and GraphPad Prism 8.0.1 software.

Quantification of HIV-1 induced CD4 T cell depletion

CD4 T cell depletion was quantified as described previously.[10] In brief, the CD4/CD8 ratio was calculated for each sample and related to the ratio of the corresponding uninfected mock sample that was set to 1.

RNP preparation

RNP complexes were prepared as described.[21] Briefly, sgRNAs were obtained from Synthego and reconstituted to 100 μM in TE buffer supplied by the manufacturer. Cas9 was obtained from IDT in a ready-to-use solution of 62 μM. SgRNA and Cas9 were mixed on ice at a ratio of 2.5:1 (sgRNA:Cas9) with PBS to obtain final concentrations of 100 pmol of sgRNA and 40 pmol of Cas9 in 50 μL complex volume, incubated for 15–20 min at RT and frozen at −80°C until usage. Immediately before nucleofection, the RNP complexes for NT Ctrl. or *cxcr4* were thawed on ice. Equal amounts of NT Ctrl. RNP and *cxcr4* RNP were used per cell in each experiment for proper comparison. The final *cxcr4* RNP mix with which cells were nucleofected further consisted of equal amounts of two different sgRNA-Cas9 RNP complexes as described.[21]

CRISPR/Cas9 RNP nucleofection of tonsil cells

Tonsil bulk cells or isolated and bead-released CD4 T cells were prepared for nucleofection as described.[21] Briefly, cells were washed once in 1xPBS and resuspended in P3 primary cell nucleofection buffer (Lonza) as recommended by the manufacturer's protocol, using $2x10^6$ cells in 20μL nucleofection buffer for 20 μL Nucleocuvette Strip or $1x10^7$ cells in 100μL for single Nucleocuvettes. Cells were mixed briefly with the RNP mix that was prepared shortly before nucleofection on ice and were transferred to the respective nucleofection cuvettes. For $2x10^6$ cells, 6 μL RNP mix in total were used while 24μL were used for $1x10^7$ cells. Lonza 4D-Nucleofector X Unit was used for electroporation and cells were immediately after resuspended in unsupplemented RPMI 1640 to reach a concentration of $4x10^7$ cells/ml and incubated for 15 min prior to dilution in tonsil medium to a final concentration of $1x10^7$ cells/ml prior to merging with non-CD4 T cells. After nucleofection, cells were cultured either in 24-well transwell or 96-well V-/F-bottom plates as indicated. Culture plate setup did not have any influence on KO efficiency.

SEB stimulation of tonsil cell cultures

SEB was added to tonsil cultures at 1μg/ml final concentration directly into the medium of V or F-bottom 96-well plates or into the lower transwell of transwell plates and was left on the cells for the remaining culture period.

Cytokine treatment of tonsil cell cultures for optimization of post-nucleofection conditions

After nucleofection of CD4 T cells, reconstituted cell suspensions were seeded in 24-well transwell plates with IL-7, IL-15 and IL-2 alone or in combination (IL-7+IL-15) at indicated concentrations of 0.5 or 2 ng/ml for IL-7 and IL-15 and 10 or 50 IU/mL for IL-2. Every 2–3 days, medium was refreshed by preparing a 3x concentrated pre-dilution of the concentrated cytokine stocks in tonsil medium which was added to fill up the lower transwells after removal of a third of the spent medium every 2–3 days.

T20 treatment of tonsil cells to inhibit fusion and entry of HIV-1

T20 (Fuzeon, Enfuvirtide) was added to the diluted virus stock for infection of tonsil cultures at 20 μM final concentration on day 7 post nucleofection, was added freshly after washing of the virus input and was renewed on day 4 post infection.

CD4 positive and negative isolation from tonsil cell suspension

In the experiment directly comparing the sorting and nucleofection efficacy in CD4 negative vs. positive sorted CD4 T cells (Figure S3), tonsil cell suspensions were processed for positive or negative CD4 T cell isolation using stemcell EasySep Human $CD4^+$ T cell Isolation Kit or EasySep Release Human CD4 Positive Selection Kit according to the manufacturer's recommendations. Briefly, tonsil cells were thawed, counted and concentration adjusted to $5x10^7$ cells/ml for negative isolation, i.e., $1x10^8$ cells/ml for positive isolation in 1xPBS with 2% FBS and 2 mM EDTA. All steps were followed according to the manufacturer's protocol, yielding an unlabeled CD4 T cell fraction from the negative isolation and a CD4 antibody and magnetic-bead labeled CD4 T cell fraction from positive isolation which underwent bead removal with the supplied release buffer directly after isolation. Purity and efficiency of the isolation procedures were assessed using CD3 and CD4 antibody staining for the negative isolation and CD3 and CD8 staining for the positive isolation as recommended. Unlabeled non-CD4 T cells resulting from the CD4 positive isolation procedure (negative fraction) were used to complement both negative and positive isolated CD4 T cells after nucleofection for the reconstituted culture in Figure S4 G-I to avoid a bias resulting from the presence of magnetic beads and possible induction of activation in cultures with negative isolated CD4 T cells and magnetic bead-labeled non-CD4 T cells. Non-CD4 T cells resulting from the positive CD4 T cell isolation were resuspended in tonsil medium, counted and resuspended at $1x10^7$ cells/ml before merging with CD4 T cells for downstream experiments.

For all experiments except the direct comparison of positive vs. negative CD4 T cell isolation, the non-CD4 T cell fraction underwent a second positive isolation procedure to deplete remaining CD4 T cells from this population or alternatively, double amounts of CD4 isolation cocktail and magnetic particles were used in the first positive isolation process in order to increase purity of the non-CD4 fraction which routinely decreased the frequency of contaminating CD4 T cells in this fraction to $1/5^{th}$ to $1/6^{th}$ of the original CD4 T cell population. After isolation, CD4 T cells were resuspended in tonsil medium, counted and processed for downstream

applications, e.g., nucleofection before resuspension at $1x10^7$ cells/ml and merging with unlabeled non-CD4 T cells at the same concentration, yielding a typical ratio of 1–4 (20%) CD4 T cells to non-CD4 T cells in the final reconstituted culture.

Celltracker staining of isolated tonsil CD4 T cells

Directly after nucleofection and incubation in unsupplemented RPMI 1640 at $4x10^7$ cells/ml, tonsil CD4 T cells were resuspended at $1x10^7$ cells/ml in celltracker DeepRed (Thermo Fisher) solution by addition of 3x volume of PBS containing 4x concentrated celltracker dye, were incubated for 15 min at 37°C and were washed in tonsil medium 2x before resuspension at $1x10^7$ cells/ml and merging with unlabeled, non-nucleofected non-CD4 T cells for reconstituted cultures.

Reactivation and expansion of EBV-specific memory CD8 T cells in tonsil tissue

Tonsils used for CD8 T cell reactivation experiments were pre-selected in separate screening experiments based on the presence of EBV-specific CD8 T cells measured by EBV peptide-specific IFNγ production compared to background activation induced by unspecific HIV-1 Gag peptides. The EBV peptide pool (EBV Peptivator, Miltenyi Biotec) contains MHC class I and class II-restricted epitopes from EBV lytic and latent cycle proteins for stimulation of CD4 and CD8 T cells, respectively. The peptides contained in the pool are recognized by most common HLA types such as HLA-A*A02:01 and HLA-B*07:02, ensuring broad response rates across different tonsil donors. The peptide mix was directly added to the culture medium at 1 μg/mL (0.6 μM for each peptide) at indicated timepoints without disturbing the cell layer and IL-7 was added at a final concentration of 1 ng/mL. Cultures were incubated for 7 days with the peptide pool and IL-7 was refreshed every 2–3 days by removing a third of the spent medium and replacing with fresh medium containing 3x concentrated IL-7. To assess IFNγ-production as a correlate for EBV-spec. CD8 T cell reactivation at designated timepoints, separate wells were exposed to the peptide pool on the start day of culture (baseline frequency of reactive CD8 T cells) and after 7 days for 30 min and subsequently incubated with Brefeldin A at 5 μg/mL final concentration for an additional 2 h to block cytokine export. Cells were then harvested with PBS +2 mM EDTA, washed with PBS and stained with zombie violet fixable viability dye and surface antibodies for human CD3, CD8, CD45RO and CD62L prior to fixation, permeabilization and intracellular cytokine staining. In every experiment, control wells that did not receive the peptide pool but were also stimulated at the end day of culture with the EBV peptide pool served as background controls for unspecific activation and expansion of CD8 T cells over the culture period that was negligible in our experiments. Further, antigen-specificity of the IFNγ production was validated in several experiments by stimulating the EBV-peptide pool cultures with an MHC class I epitope pool derived from HIV-1 Gag peptides in parallel, to which the healthy donors in our experiments did not respond with IFNγ production (example S1 J).

QUANTIFICATION AND STATISTICAL ANALYSIS

Statistical analysis of datasets was carried out using Prism version 8.0.1 (GraphPad). Normality was tested using Shapiro-Wilk test and statistical significance was calculated using the appropriate tests for paired data. For normally distributed data, statistical significance was calculated using paired t-test for comparison of two conditions or repeated measures (RM) one-way ANOVA with Holm-Sidak's multiple comparison test for comparison of more than two conditions. For not normally distributed data, Wilcoxon test was used for comparison of two conditions with one being a control condition or Friedman test with Dunn's multiple comparison test for comparison of more than two conditions as indicated. n.s., not significant; *, $p < 0.05$; **, $p < 0.01$; ****, $p < 0.0001$. See figure legends for details.

Cell Reports Methods, Volume *4*

Supplemental information

Activation-neutral gene editing of tonsillar CD4 T cells for functional studies in human *ex vivo* tonsil cultures

Katharina Morath, Lopamudra Sadhu, Gerhard Dyckhoff, Madeleine Gapp, Oliver T. Keppler, and Oliver T. Fackler

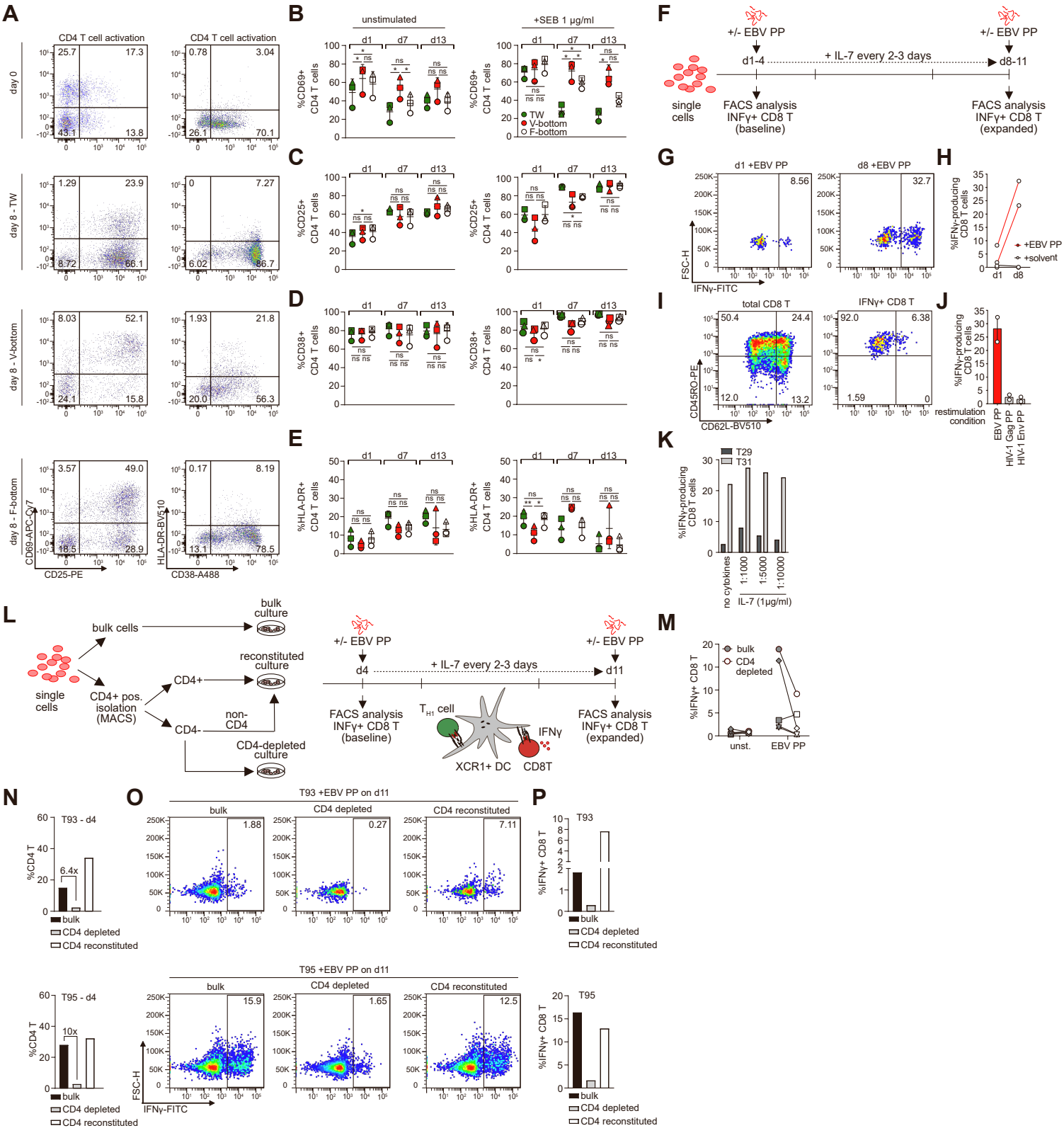

Morath et al. 2023, Fig. S1, related to Fig. 1 and Fig.2

Figure S1. Tonsil CD4 T cells can respond to superantigen and provide antigen-specific help to memory CD8 T cells. Related to Figure 1 and Figure 2. (A) Representative dot plots of CD4 T cell surface activation marker expression showing frequency of cells positive for CD25 and CD69 (left panel) or CD38 and HLA-DR (right panel) on day 0 and day 8 of culture as indicated with (+SEB 1 µg/ml) exogenous activation in transwell, V- or F bottom plate culture. (B)-(E) Quantification of A without (left panel) or with (right panel) exogenous activation for three tonsils in TW (green), V-bottom (red) or F-bottom (white) setups. Shown are means with SD. Each symbol represents one donor. Statistical significance was assessed by repeated measures one-way ANOVA for all datasets except for CD25 expression in unstimulated condition in C, where data was not normally distributed and Friedman test was used (ns, $p>0.05$; *, $p<0.05$; **, $p<0.01$; ***, $p<0.001$; ****, $p<0.0001$). (F) Schematic of the experimental set-up for assessment of EBV-specific memory CD8 T cell reactivation in tonsil culture as in Fig. 2G. (G) Representative dot plots of tonsil CD8 T cells showing IFNγ-production upon EBV peptide stimulation on day 1 (baseline) and day 8 (expanded). (H) Quantification of G for two tonsils, showing increase of EBV-specific CD8 T cells that are identified by IFNγ-production over the culture period. Solvent control is water. (I) Representative dot plots of tonsil CD8 T cells after stimulation with EBV peptide pool, showing typical distribution of memory subsets among total or IFNγ+ tonsil CD8 T cells measured by CD45RO and CD62L expression, confirming an effector memory phenotype of the reactivated CD8 T cell response. (J) Quantification of IFNγ-production among CD8 T cells after 7 days of culture with EBV peptide pool and upon restimulation with EBV peptide pool or unspecific/background IFNγ-production upon restimulation with HIV-1 Gag and HIV-1 Env peptide pools, validating EBV-specificity of the expansion and reactivation process. (K) Quantification of IFNγ+ CD8 T cells upon restimulation with EBV peptide pool after 7 days of culture with EBV peptide pool and additional supplementation of IL-7 at indicated concentrations for two tonsils, respectively. (L) Schematic of the experimental set-up for assessment of CD4 T cell help to EBV-specific memory CD8 T cell reactivation. Briefly, tonsil single cell suspensions were seeded as bulk cultures or subjected to CD4 T cell positive isolation and the CD4-depleted fraction was seeded with or without reconstitution of CD4 T cells. The cultures were stimulated with EBV peptide pool on day 4 and expansion was assessed 7 days later. (M) Quantification of IFNγ+ CD8 T cells on day 11 after 7 days of culture with (EBV PP) or without (unst) EBV peptide pool for bulk cultures (grey) or CD4-depleted cultures (white). Each symbol represents one donor. (N) Frequency of CD4 T cells among tonsil cells upon initial peptide stimulation on day 4 for bulk, CD4-depleted and CD4-reconstituted cultures for two tonsils, respectively. (O) Dot plots showing IFNγ-production of tonsil CD8 T cells upon EBV peptide pool restimulation on day 11 after 7 days of culture with EBV peptide pool for bulk, CD4-depleted and CD4-reconstituted cultures for the two tonsils from N. (P) Quantification of O for the two tonsils. Cells in F-P were cultured on F-bottom plates.

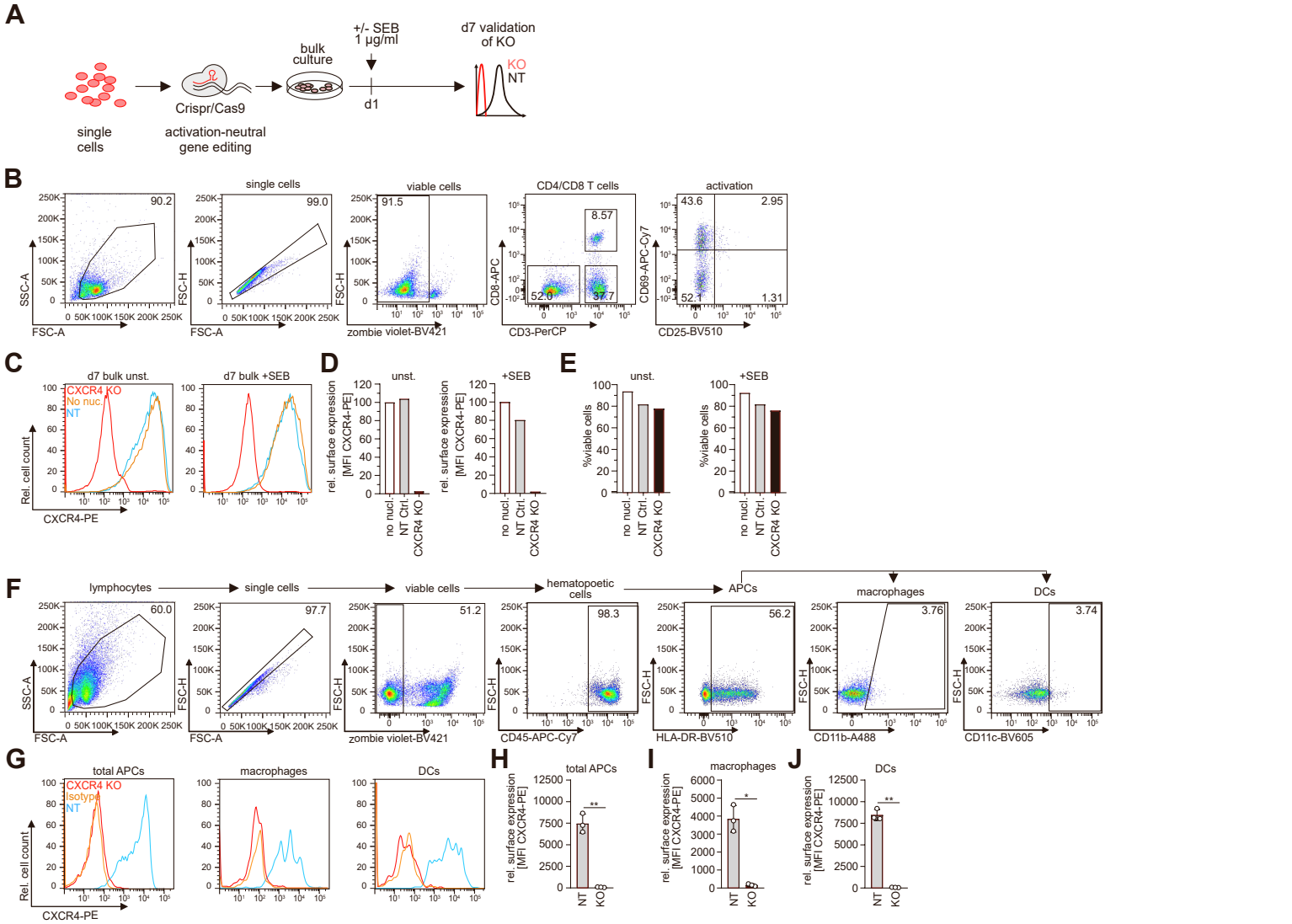

Morath et al. 2023, Fig. S2, related to Fig, 3

Figure S2. Crispr/Cas9 KO of bulk tonsil cells does not require exogenous activation and is efficient across APCs and myeloid cell populations. Related to Figure 3. (A) Schematic of the experimental set-up. (B) Representative dot plots showing gating strategy and typical activation phenotype of tonsil CD4 T cells upon seeding in the absence of exogenous activation, measured by CD25 and CD69 expression. (C) Histograms showing CXCR4 surface expression on CD4 T cells in tonsil bulk cultures without (left) or with (right) SEB stimulation at 1 µg/ml on day 7 post nucleofection. SEB was added 1 day post nucleofection. Superimposed are histograms for the non-targeting control (NT) and no nucleofection (no nucl.) condition. (D) Quantification of C for one tonsil without (unst.) or with (+SEB) exogenous activation on day 7 post nucleofection. (E) Frequency of viable CD4 T cells for conditions in C. Cells in A-E were cultured in 24-well TW-plates. (F) Representative dot plots and gating strategy for identification of myeloid subsets among tonsil cell cultures. (G) Representative histograms showing CXCR4 surface expression on total APCs, macrophages or dendritic cells (DCs) on day 7 post nucleofection with CXCR4-targeting RNP (CXCR4 KO) with superimposed histograms for the non-targeting RNP (NT) condition and isotype control. (H)-(J) Quantification of G for NT or CXCR4 KO in total APCs, macrophages or DCs. Cells were cultured in 96-well F-bottom plates. Each dot represents one tonsil. Shown are means with SD. Statistical significance was assessed by paired t-test (ns, $p>0.05$; *, $p<0.05$; **, $p<0.01$; ***, $p<0.001$; ****, $p<0.0001$).

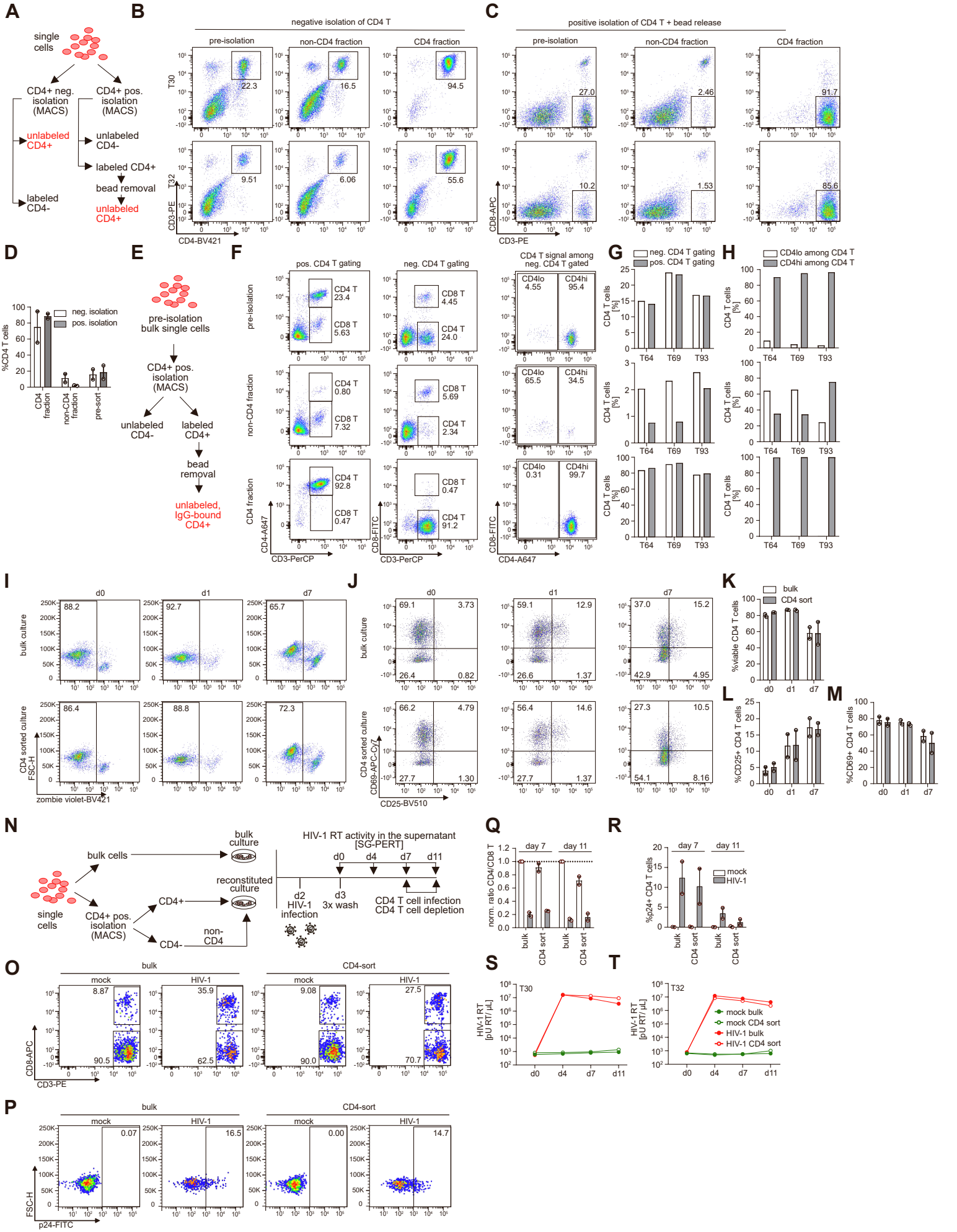

Morath et al. 2023, Fig. S3, related to Fig. 4

Figure S3. Positive isolation of tonsil CD4 T cells is efficient and does not affect phenotype or functionality. Related to Figure 4. (A) Schematic of the experimental set-up for CD4 T cell positive or negative isolation for comparison of sorting efficiency with indicated fractions resulting from the two procedures. (B) and (C) Dot plots of CD4 negative (B) or positive (C) isolation fractions before (pre-isolation) and after sorting (non-CD4 fraction and CD4 fraction) for two tonsils. Indicated are frequencies of CD4 T cells based on CD3 and CD4 surface staining for negative isolation (B) or CD3 and CD8 surface staining for positive isolation (C). (D) Quantification of B and C for the two tonsils. Shown are means with range. Each dot represents one tonsil. (E)-(H) Assessment of the residual CD4 T cells left in the non-CD4 T cell fraction after positive isolation. (E) Schematic of the experimental set-up for positive isolation, indicating the resulting populations of antibody-bound, bead-released CD4 T cells and unlabeled non-CD4 T cells. (F) Representative dot plots showing tonsil cells pre-isolation, the non-CD4 T cell fraction post-isolation and CD4 T cell fraction post-isolation stained with CD3, CD8 and CD4 antibodies but showing either positive CD4 T cell gating based on CD3 and CD4 staining (left panel) or negative CD4 T cell gating based on CD3 and CD8 staining (middle panel). The right panel shows CD4 signal among negatively gated CD4 T cells based on CD3 and CD8 staining in the indicated fractions pre- and post-isolation. The CD4 antibody that was used in this experiment is the OKT4 clone which has a distinct binding site from the CD4-binding antibodies used in the positive isolation procedure. (G) Quantification of left and middle panel in F, indicating frequency of CD4 T cells based on the two gating strategies in the same samples. (H) Quantification of the right panel in F, indicating true frequency of CD4-positive cells among negatively gated CD4 T cells. (I)-(M) Validation of the activation-neutral CD4 T cell positive isolation procedure. (I) and (J) Representative dot plots showing viability (I) or activation (J) by surface expression of CD25 and CD69 of CD4 T cells on day 0, day 1 or day 7 in untouched bulk cultures or after CD4 T cell positive isolation and reconstitution of the culture. (K)-(M) Quantification of I and J for two tested tonsils at the respective timepoints. Shown are means with range. Each dot represents one tonsil. (N) Schematic of the experimental workflow to assess impact of the CD4 positive isolation on HIV-1 infection dynamics. Briefly, tonsil cells were thawed and infected with HIV-1 NL4.3SF2Nef at $1.5x10^5$ BCU per $2x10^6$ cells one day after CD4 positive isolation and reconstitution or bulk culture seeding. On the following day (d0), cells were washed 3x and infection was assessed by analysis of CD4 T cell infection and depletion by flow cytometry analysis upon final harvest. Further, production of HIV-1 virions in the supernatant was measured by SG-PERT throughout the infection course. (O) and (P) Representative dot plots showing CD4 and CD8 T cells subgated from CD3 T cells (O) as well as p24 signal in CD4 T cells (P) in bulk or CD4 T cell-sorted mock or HIV-1 infected conditions, respectively on day 7 post infection. (Q) and (R) Quantification of O and P for two tonsils with the ratio of CD4 vs. CD8 T cells in Q normalized to the mock condition for the respective bulk cultures. Shown are means with range. Each dot represents one tonsil. (S) and (T) HIV-1 RT activity in the supernatant of mock or HIV-1 infected bulk or CD4 T cell-sorted cultures at indicated timepoints for the two tonsils from O-R, respectively. Cells in I-T were cultured in 24-well TW-plates.

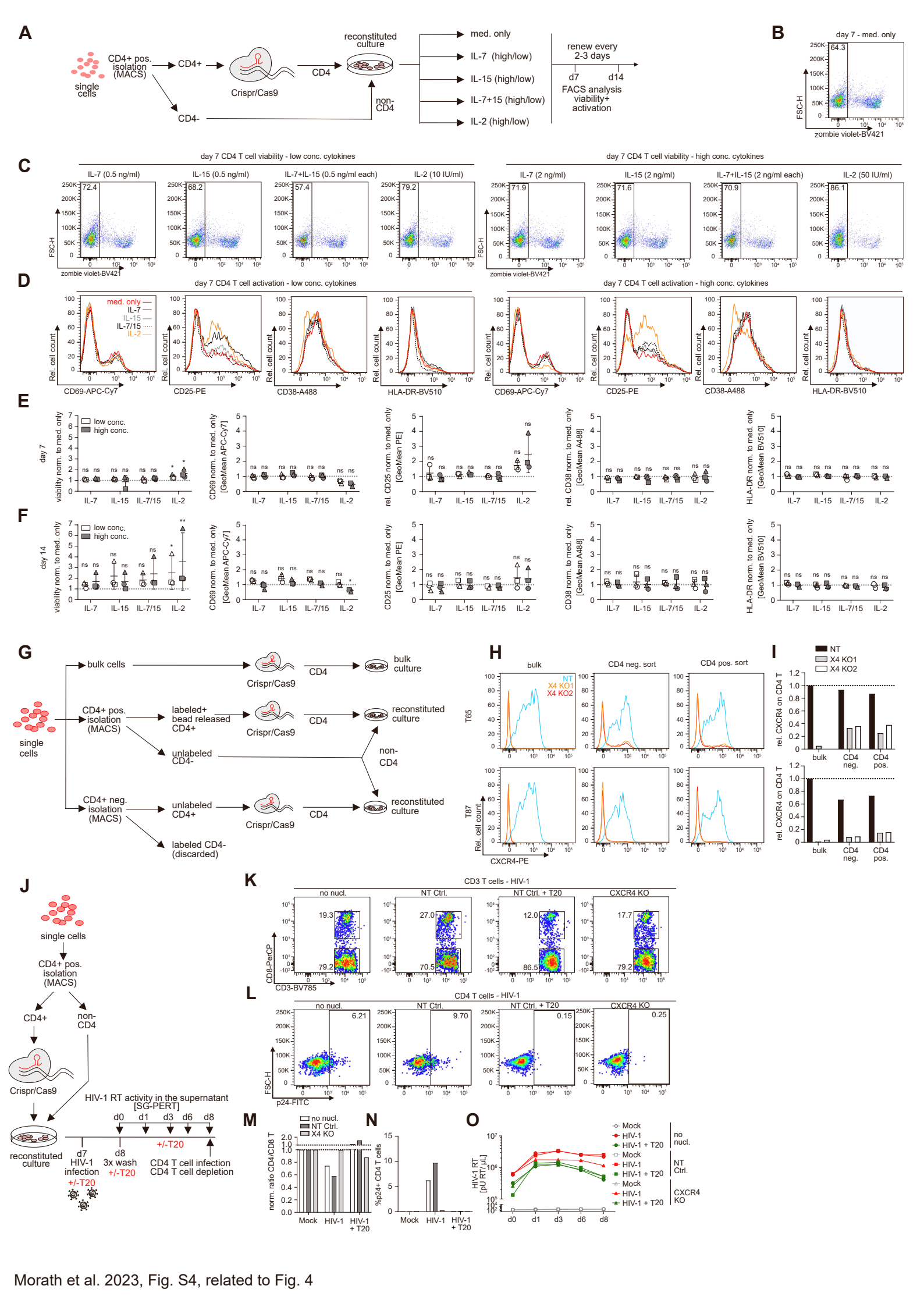

Morath et al. 2023, Fig. S4, related to Fig. 4

Figure S4. Crispr/Cas9 KO of tonsil CD4 T cells is highly efficient independent of the isolation strategy or RNP preparation and cytokine supplementation of the culture post KO is not required. Related to Figure 4. (A) Schematic of the experimental workflow. Briefly, tonsil cells were thawed, CD4 T cells were sorted, nucleofected with NT Ctrl. RNP and merged with non-CD4 T cells and cultured in transwell plates. Reconstituted cultures were kept in tonsil medium without further supplements (med. only) or with IL-7, IL-15 (separate or in combination) or with IL-2 with a low or high concentration as indicated. (B) and (C) Representative dot plots of the med. only (B) or cytokine-supplemented cultures with low (left panel) or high (right) concentrations on day 7 showing viability of the CD4 T cells based on zombie violet staining. (D) Representative histograms of CD4 T cells showing surface expression of activation markers CD25, CD69, CD38 or HLA-DR in low (left panel) or high (right panel) cytokine conditions. Superimposed are histograms for the med. only, IL-7, IL-15, IL-7+IL-15 or IL-2 cultures as indicated. (E) and (F) Quantification of C and D for day 7 (E) or day 14 (F) of culture. For each donor, values were normalized to the med. only condition. Each symbol represents one donor. Shown are means with SD. Statistical significance was assessed by Friedman test for normalized data in E and F (ns, $p>0.05$; *, $p<0.05$; **, $p<0.01$; ***, $p<0.001$; ****, $p<0.0001$). (G) Schematic of the experimental set-up for determining nucleofection efficiency in bulk or CD4 negatively vs. positively-isolated CD4 T cells. Briefly, tonsil cells were thawed and either nucleofected as bulk cultures or processed for CD4 negative or CD4 positive isolation with subsequent bead release. CD4 T cells resulting from the two separation procedures were nucleofected and merged with the unlabeled, CD4-depleted fraction resulting from the CD4 positive isolation while labeled non-CD4 T cells resulting from the CD4 T cell negative isolation were discarded. (H) Histograms showing CXCR4 surface expression on CD4 T cells in either bulk nucleofected cultures or CD4 negatively and CD4 positively-isolated and nucleofected populations on day 7 post nucleofection for two tonsils. Two individually prepared RNP complexes (X4 KO1 and X4 KO2) were tested side by side in each condition to test for variability of the complex quality in addition to CD4 T cell sorting strategy and to estimate overall robustness of the workflow. Superimposed are histograms for the respective non-targeting control (NT) condition. (I) Quantification of CXCR4 surface levels on CD4 T cells as shown in H for the two tested tonsils and the two RNP preparations normalized to the bulk NT values for each tonsil. Cells were cultured in 96-well plates. (J)-(O) Validation of the inhibitory effect of CXCR4 KO in CD4 T cell sorted cells in the context of HIV-1 infection by comparison with T20 entry inhibitor of HIV-1. Data is derived from the same experiment and donor as shown in Figure 4 G and H as T20 inhibition was tested in parallel, hence the controls are identical. Briefly, tonsil CD4 T cells were positively isolated, nucleofected and after 7 days, infected with HIV-1 NL4.3SF2Nef at $1.5x10^5$ BCU per $2x10^6$ cells in the presence or absence of T20/Enfuvirtide throughout the culture period. (K) and (L) Dot plots showing CD4 and CD8 T cells subgated from CD3 T cells (K) as well as p24 signal in CD4 T cells (L) on day 8 post infection in the non-nucleofected condition or NT Ctrl (untreated or with T20 treatment) or CXCR4 KO condition as indicated. (M) and (N) Quantification of K and L for one tonsil with the ratio of CD4 vs. CD8 T cells in M normalized to the mock condition for the respective conditions. (O) HIV-1 RT activity in the supernatant of mock or HIV-1 infected CD4 T cell-sorted cultures for the different conditions at indicated timepoints for one tonsil. Cells in J-O were cultured in 24-well TW-plates.

		pre-isolation			post-isolation			
		Starting total cell count	**% non-CD4 T (cell count)**	**% CD4 T (cell count)**	**total cell count selected fraction**	**% CD4 T in selected fraction**	**Total cell count non-selected fraction**	**% residual CD4 T in non-selected fraction**
CD4 negative isolation	**T30**	2,50E+07	77,7 (1,94E+07)	22,3 (5,58E+06)	2,85E+06	94,5	NA	NA
	T32	2,50E+07	90,5 (2,26E+07)	9,5 (2,38E+06)	1,50E+06	55,6	NA	NA
	T65	1,25E+07	86,3 (1,08E+07)	13,7 (1,71E+06)	3,38E+06	43,6	NA	NA
	T87	1,25E+07	78,9 (9,86E+06)	21,1 (2,64E+06)	2,69E+06	66,9	NA	NA
CD4 positive isolation	**T30**	4,73E+07	72,5 (3,43E+07)	27,5 (1,30E+07)	7,91E+06	91,3	2,74E+07	2,4
	T32	5,00E+07	89,9 (4,50E+07)	10,1 (5,05E+06)	3,29E+06	85,5	3,36E+07	1,5
	T65	2,50E+07	85,5 (2,14E+07)	14,5 (3,63E+06)	1,70E+06	90,5	1,13E+07	2,2
	T87	2,50E+07	76,3 (1,91E+07)	23,7 (5,93E+06)	2,50E+06	91,5	1,06E+07	3,7

Table S1. Comparison of cell yields and population purity obtained from positive or negative isolation of tonsil CD4 T cells. Related to Figure 3. Table summarizing cell yields from negative and positive isolation performed in parallel with starting material from the same tonsils as indicated. Frequency of CD4 and non-CD4 T cells is based on flow cytometry analysis following CD3 and CD4 staining for negative isolation or CD3 and CD8 staining for positive isolation, respectively.